Weissel, J., Peirce, J., Taylor, E., Alt, J., et al., 1991
Proceedings of the Ocean Drilling Program, Scientific Results, Vol. 121

4. PLANKTONIC FORAMINIFER FAUNAL VARIATIONS IN THE NORTHEASTERN INDIAN OCEAN: A HIGH-RESOLUTION RECORD OF THE PAST 800,000 YEARS FROM SITE 758[1]

Min-Te Chen[2] and John Farrell[2]

ABSTRACT

We present a high-resolution (6 k.y. sample interval) record of planktonic foraminifer faunal variations for the past 800 k.y. from ODP Site 758 in the northeastern Indian Ocean. The record is examined within the context of a coarse fraction stratigraphy which is a lithologic index of $CaCO_3$ preservation, and an oxygen isotope stratigraphy which provides a chronostratigraphy and a record of climate change. Variations in the relative abundance of 27 planktonic foraminifer species primarily reflect fluctuations in the intensity of $CaCO_3$ dissolution. $CaCO_3$ dissolution covaries with climate fluctuations at a cyclicity of about 100 k.y. Glacial-aged sediments are generally well preserved, as indicated by faunal and lithologic indices. Interglacial-aged sediments show poorer preservation. The ~100-k.y. cycles are superimposed upon the long-term Brunhes Dissolution Cycle. This cycle is characterized by an interval of poor preservation centered between 400 and 550 ka and is bounded by good preservation events at 25 and 750 ka. Ecological factors also control variations in the foraminifer fauna. Changes in ecology are inferred from downcore fluctuations in the relative abundances of foraminifer species that have a similar level of resistance to dissolution. We focus on three species (*Neogloboquadrina dutertrei, Pulleniatina obliquiloculata, Globorotalia menardii*) with a relatively high resistance to dissolution. The long-term increase in *N. dutertrei* since at least 800 ka is interpreted as either a gradual decrease in the sea-surface salinity, or an increase in the biogenic productivity of the surface waters. These factors may be controlled by the strength of the monsoon climate. Extremely high abundances of *P. obliquiloculata* are observed in certain downcore intervals and are interpreted as times when the surface water conditions in the northeast Indian Ocean were similar to those in the modern western tropical Pacific, but not the modern Indian Ocean.

INTRODUCTION

A major objective of Ocean Drilling Program (ODP) Leg 121 is the investigation of Neogene climate and ocean history in the Indian Ocean. A significant portion of this history is recorded in planktonic foraminifers. Climate and ocean change is recorded by variations in faunal composition, by fluctuations in the chemical composition of foraminifer skeletons, and by the preservation state of foraminifers. With faunal information, we can evaluate the ecological response to climatically-induced changes in surface water conditions. Faunal assemblages also reflect the preservation state of $CaCO_3$ on the seafloor which documents fluctuations in the intensity of $CaCO_3$ dissolution, and thus changes in abyssal water chemistry.

The sedimentary section recovered at ODP Site 758, located in the northeastern Indian Ocean (Fig. 1), provides an excellent opportunity to study oceanic and climatic change. The Quaternary section was recovered in multiple advanced piston cores (APC) as a continuous and undisturbed sequence which accumulated at an average rate of 1.6 cm/k.y. (Farrell and Janecek, this volume). The specific objectives of this study are to: (1) document variations in the relative abundance of planktonic foraminifer species in late Quaternary sediments (0–800 ka); (2) determine the timing and magnitude of faunal change; and (3) identify the ecological and preservational processes which affected the assemblages.

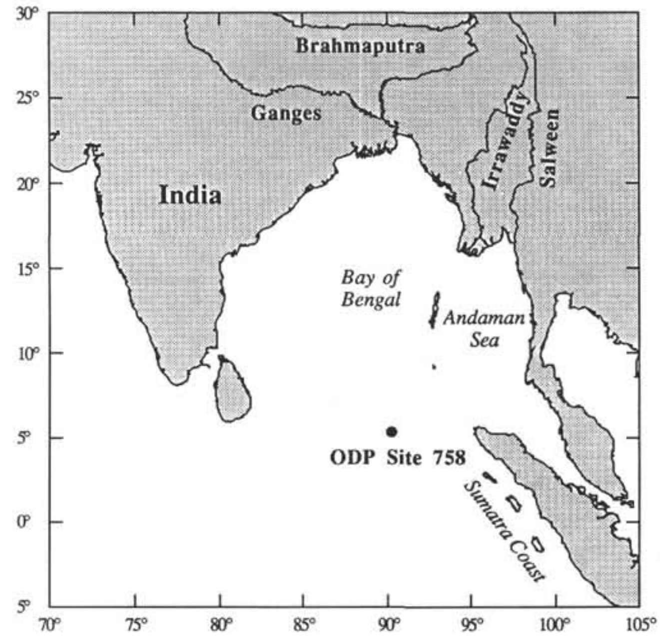

Figure 1. Location of ODP Site 758 in the northeastern Indian Ocean.

REGIONAL SETTING

Site 758 was drilled at 5°23.05′N, 90°21.67′E in a water depth of 2924 m (Fig. 1). The site is located at the southernmost end of the Bay of Bengal, atop the Ninetyeast Ridge, at least 1000 m above the Bengal Fan. This fan is the world's largest, and it is built of terrigenous sediments carried from the Himalayan region by the Ganges-Brahmaputra, Irrawaddy, and Salween river systems to the Bay of Bengal (Curray and Moore, 1971; Goldberg and Griffin, 1970). The Quaternary sediments at Site 758 are predominantly biogenic calcareous ooze with secondary amounts of terrigenous clay and occasional intercalated volcanic ash layers (Shipboard Scientific Party, 1989).

[1] Weissel, J., Peirce, J., Taylor, E., Alt, J., et al., 1991. *Proc. ODP, Sci. Results,* 121: College Station, TX (Ocean Drilling Program).
[2] Department of Geological Sciences, Brown University, Providence, RI 02912-1846, U.S.A.

The oceanography and climatology of the North Indian Ocean are strongly controlled by the monsoon climate regime which is characterized by the seasonal reversal of wind and surface water circulation. In the northern Bay of Bengal, the surface waters undergo dramatic changes in salinity associated with the monsoon. During the summer months (May–October), strong southwesterly winds transport large quantities of water vapor to the Indian subcontinent. Much of the water precipitated over land is carried to the Bay of Bengal by the river systems. In the winter months (November–April), dry winds blow from the northeast. The volume of water discharged into the Bay of Bengal from the Ganges-Brahmaputra and Irrawaddy river systems during the summer is five times greater than during the winter (Rodolfo, 1967). The variation in fresh water input to the Bay of Bengal produces a seasonal salinity gradient in the surface waters. During the summer monsoon, a steep salinity gradient, increasing to the south, exists along 90°E (Wyrtki, 1973). This gradient forms primarily in response to riverine input, but is enhanced by the Southwest Monsoon Current which carries high salinity water into the central Bay of Bengal from the equatorial Indian Ocean (Prell et al., 1980). Sea-surface temperature (SST) variations in the Bay of Bengal are nearly constant over the year when compared to the fluctuations observed in the Arabian Sea (Wyrtki, 1973). During the winter monsoon, the average temperatures in the Bay of Bengal range from 26°C in the north, to 28°C in the south. During the summer monsoon, the temperatures are slightly higher and nearly isothermal, ranging from 28°C to 29°C (Wyrtki, 1973). In the southernmost reaches of the Bay of Bengal, the SST and the salinity show little variation throughout the year. In this region, near Site 758, the SST is 28.5±1.0°C and the salinity is 33.8±0.3‰ throughout the year (Wyrtki, 1988). These values are typical of open ocean tropical regions.

Little is known about monsoon induced variations in biological productivity in the Bay of Bengal. Only in isolated locations within the Andaman Sea have distinct biological responses to monsoonal induced upwelling been documented (Colborn, 1975). During the late Quaternary, variations in biological productivity in the Andaman Sea have been related to the strength of the Northeast winter Monsoon (Fontugne and Duplessy, 1986). The variation of productivity recorded at Site 758 would largely depend on the Northeast Monsoon strength and associated equatorial current intensity.

METHODS AND DATA

Stratigraphy

Since sediment recovery gaps as large as 2.7 m occurred between almost every advanced piston core at Site 758, a composite depth section was constructed (Farrell and Janecek, this volume) by splicing together sedimentary intervals from Holes 758A and B based on detailed correlations of high resolution stratigraphies such as magnetic susceptibility. The composite depth section provides a continuous record of the sedimentary sequence at Site 758. We used samples from Cores 121-758A-1H and -2H which had recovery percentages of 102% and 104%, respectively. A sedimentary interval of approximately 1.42 m representing approximately 60 k.y. is missing between the two cores (see Fig. 4 in Farrell and Janecek, this volume). This gap, which contains oxygen isotope stage 10 (using the nomenclature of Imbrie et al., 1984), is successfully patched with the equivalent sedimentary interval from Core 121-758B-1H.

The chronostratigraphy used in this study is from Farrell and Janecek (this volume) and is primarily based on the correlation of the Site 758 oxygen isotope record from the planktonic foraminifer *Globigerinoides sacculifer* (300–355 μm size fraction) to the global average oxygen isotope record, the Spectral Mapping (SPECMAP) stack (Imbrie et al., 1984; Prell et al., 1986). Age control is also provided by the position of the Brunhes/Matuyama paleomagnetic chron boundary (at 10.75 meters below sea floor (mbsf) which corresponds to 12.17 m on the composite depth scale). Our chronostratigraphy is consistent with the age constraints provided by the biostratigraphic datums established onboard (Shipboard Scientific Party, 1989) and with the disappearance of the pink variety of *Globigerinoides ruber* at 120 ka (Thompson et al., 1979) which occurs between Samples 121-758A-1H-2, 131 cm and 121 cm.

Faunal Analysis

The 134 faunal samples used in this study are aliquots from the same samples used to determine %$CaCO_3$, coarse fraction, and stable isotope composition (Farrell and Janecek, this volume). The samples have an average spacing of 10 cm, which is equivalent in time to 6 k.y. The samples span from the core top (0.01 m) down to 13.83 m which corresponds to an age interval of 0–800 ka. Preparation of the samples from the initial stages up to and including the separation of the >150 μm size fraction is described in Farrell and Janecek (this volume). Subsequent sample preparation and analysis follows the method outlined in Imbrie and Kipp (1971). Each sample is a split of the >150 μm fraction. Of the 134 samples, 124 contain at least 300 whole foraminifers. The remaining 10 samples have experienced greater dissolution and thus contain between 200 and 300 whole foraminifers. The relative abundances of 27 species of planktonic foraminifers were calculated for each sample and are listed in Table 1. The taxonomy of planktonic foraminifers used in this study is based on Parker (1962), Bé (1967), and Kipp (1976). This taxonomy was also used in previous studies of late Quaternary Indian Ocean foraminifers (e.g., Cullen, 1981; Cullen and Prell, 1984).

RESULTS

Relative Abundance of Planktonic Foraminifers

Descriptive statistics (Table 2) show that over the past 800 k.y., the foraminifer assemblages are dominated by six species which constitute 76% of the total planktonic foraminifer composition. In order of decreasing mean abundance, the six species are: *G. ruber*, *Pulleniatina obliquiloculata*, *Neogloboquadrina dutertrei*, *Globorotalia menardii*, *G. sacculifer*, and *Globigerinita glutinata*. These six species show larger downcore variations than the other species, as indicated by the larger standard deviations of the six.

Variations in the abundance of these six dominant species in the tropical Indian Ocean have previously been attributed to $CaCO_3$ preservation and ecological factors (Cullen and Prell, 1984). *G. ruber* and *G. sacculifer* are major components of surface sediments underlying the warm waters of tropical oceans and are highly-susceptible to $CaCO_3$ dissolution. *G. glutinata* is moderately-susceptible to dissolution, and is a dominant component in assemblages from regions influenced by upwelling, such as the western Arabian Sea and the northeastern Bay of Bengal (Cullen and Prell, 1984). The ecological role of this species is not well understood but it may be an ecotone between upwelling and tropical faunal assemblages (Hutson and Prell, 1980), or it may be associated with the margins of upwelling zones (Prell et al., 1990). *P. obliquiloculata*, *N. dutertrei*, and *G. menardii* are tropical species generally considered to be more resistant to dissolution (Berger, 1968; 1979; Parker and Berger, 1971; Adelseck, 1978; Thunell and Honjo, 1981a; b). *N. dutertrei* and *G. menardii* are highly abundant in regions characterized by a relatively shallow thermocline, intense upwelling, and high productivity (Fairbanks et al., 1982; Thunell and Reynolds, 1984). These species are especially abundant in strong current systems near continental margins (Bé and Tolderlund, 1971). The ecological niche of *P. obliquiloculata* is unclear. The high abundance of this species in the western-central tropical Pacific suggests that it prefers relatively warmer SST and/or a depressed thermocline. Nevertheless, in samples from the tropical Atlantic Ocean (Ravelo et al., 1990), this species occurred with *N. dutertrei* and *G. menardii* which prefer a shallow thermocline.

Globigerina bulloides and *Globorotalia tumida* are relatively minor but important components of the foraminifer assemblages because respectively, they are strongly linked to ecological and preservational conditions. *G. bulloides* is an important component of subpolar-transitional faunas (Parker and Berger, 1971; Kipp, 1976; Hutson and Prell, 1980) and is abundant in low latitude upwelling regions such as the Arabian Sea (Hutson and Prell, 1980; Prell and Curry, 1981; Prell, 1984; Cullen and Prell, 1984). *G. tumida* is most abundant in samples from the deepest waters and is quite rare in shallow water sites (Cullen and Prell, 1984). This observation is consistent with the conclusion that *G. tumida* is one of the most dissolution-resistant foraminifer species (Berger, 1968; 1979; Parker and Berger, 1971; Adelseck, 1978; Thunell and Honjo, 1981a; b).

Temporal Variation of Planktonic Foraminifers

The relative percentages of the species in the core top sample (121-758A-1H-1, 1 cm) from Site 758 are quite similar to percentages observed in nearby surface sediment samples (Cullen and Prell, 1984). Downcore faunal assemblages at Site 758 can be interpreted with respect to assemblages from modern sediments (Cullen and Prell, 1984; Prell, 1985) because of the similarity in core top results. Fluctuations in relative abundance of eight major foraminifer species are presented with respect to age (Fig. 2). The eight species include *G. bulloides* and *G. tumida*, in addition to the six dominant species previously discussed. Particularly noteworthy among the trends shown in Figure 2 are:

1. The pulse of decreased abundances of *G. ruber*, *G. sacculifer*, *G. bulloides*, and *G. glutinata* between 490 and 550 ka, and the concomitant increase in the abundance of *P. obliquiloculata*, *G. menardii*, and *G. tumida*.
2. A long-term cycle in *G. tumida* abundance characterized by low values from 700 to 800 ka and from 0 to 10 ka, and high values centered between 400 and 550 ka.
3. Intervals, such as between 490 and 550 ka, in which the abundance of *P. obliquiloculata* was much greater than the maximum value of 21% observed in surface sediments of the North Indian Ocean (Cullen and Prell, 1984).

Temporal Variations in the Resistant Species Ratio (RSP%)

Variations in foraminifer assemblages reflect changes in preservation on the sea floor, as well as ecological changes at the sea surface. The preservation of planktonic foraminifers in the deep sea is controlled by the saturation state of the bottom waters and the interstitial pore waters with respect to calcium carbonate, which in turn is a function of overall mixing rate and fertility (Berger, 1979). Quantitative (Thunell and Honjo, 1981a; b) and semi-quantitative (Adelseck, 1978; Berger, 1968; 1979; Parker and Berger, 1971; Malmgren, 1983; Peterson and Prell, 1985a) field and laboratory studies have established a relative ranking of the degree to which planktonic foraminifer species are susceptible to $CaCO_3$ dissolution. For example, in surface sediments from the eastern equatorial Indian Ocean, Peterson and Prell (1985a) observed a systematic increase in the abundance of foraminifer species with thick skeletons, such as *G. menardii*, *G. tumida*, and *N. dutertrei*, with increasing water depth. The abundance of the dissolution resistant species increases at the expense of less resistant species. In deep water samples, the assemblage contains a reduced number of specimens from the species which are moderately-susceptible to dissolution, such as *G. glutinata*, *N. hexagona*, *G. bulloides*, and *G. calida*, and even fewer specimens of the highly-susceptible species such as *G. ruber* and *G. sacculifer*.

The foraminifer lysocline (FL) is the water depth which separates well-preserved from poorly-preserved foraminifer assemblages (Berger, 1975). The depth of the FL in the Indian Ocean has been determined quantitatively based on noticeable changes in the resistant species ratio (RSP) (Cullen and Prell, 1984). The RSP% is defined (Cullen and Prell, 1984) as the sum of the percentages of the following 14 dissolution-resistant species and varieties: *G. menardii*, *N. dutertrei*, *P. obliquiloculata*, *G. tumida*, *S. dehiscens*, "pachyderma-dutertrei" intergrade, *G. crassaformis*, *G. menardii neoflexuosa*, *G. pachyderma* right coiling, *G. truncatulinoides* right coiling, *G. pachyderma* left coiling, *G. inflata*, *G. truncatulinoides* left coiling, and *G. humilis*. In our calculation of the RSP%, we grouped *G. menardii neoflexuosa* with *G. menardii*, and we excluded *G. pachyderma* left coiling and *G. humilis* because they are absent from the assemblages. The FL has been equated with the water depth where the RSP level is equal to 30% (Cullen and Prell, 1984). Values greater than 30% are considered to lie beneath the FL. Consistent with the original definition of RSP%, the variations in faunal assemblages with RSP% greater than 30% are considered to be significantly influenced by $CaCO_3$ dissolution. Assemblages with RSP% values less than 30% lie above the FL and variations in these assemblages are thought to primarily reflect fluctuations in foraminifer input from the surface waters, and thus ecological factors. Nevertheless, some dissolution does occur above the FL (Peterson and Prell, 1985a). In the Bay of Bengal, the FL deepens from ~2200 m in the northernmost regions, to 2750 m in the south (Cullen and Prell, 1984). According to this estimate, the depth of Site 758 (2924 m) is presently located slightly below the FL. This estimate is consistent with the Site 758 core top RSP value of 36%.

In Figure 3, the RSP% of the samples from Site 758 is compared to the coarse fraction and to $\delta^{18}O$. Coarse fraction is defined as the wt% of a sample >150 mm. Coarse fraction is a reliable index of relative dissolution intensity in many regions (Berger, 1970; Berger et al., 1982). Furthermore, since coarse fraction is a lithologic index rather than a faunal index, it is an independent proxy indicator of dissolution. Low coarse fraction values are interpreted as times of enhanced dissolution. The oxygen isotope record is a proxy indicator of global ice volume (Shackleton and Opdyke, 1973; 1976) and is thus used to identify glacial and interglacial climate stages (Imbrie et al., 1984; Prell et al., 1986). As expected, a negative correlation exists between RSP% and coarse fraction (Fig. 4) since dissolution is thought to control both parameters. The correlation is noisy for several reasons. First, RSP% is controlled by ecological factors as well as by dissolution. Second, RSP% is probably more sensitive than coarse fraction to subtle changes in the corrosiveness of the water. If this is the case, the dissolution response of RSP% would lead the coarse fraction response. In addition, the magnitude of the RSP% response is not necessarily equal to the magnitude of the coarse fraction response. The increase of RSP% in the downcore sample is mainly attributed to the increase of differential solution of foraminifer assemblages. The most severe dissolution is indicated by the highest RSP% and the lowest coarse fractions. Likewise, the best preservation is indicated by the lowest RSP% and the highest coarse fractions. Using the narrow definition of the FL as the 30% RSP level, the downcore RSP% results indicate that Site 758 has remained beneath the FL during most of the past 800 ka. The only times during which the FL deepened to or below the depth of Site 758 (2924 m) was during the latter half of glacial stages and during transitions from glacials to interglacials. For example, the

Table 1. Planktonic foraminifer percentage data in the composite depth section from Hole 758A. Foraminiferal codes are listed in Table 2.

Core, section interval (cm)	Composite depth (m)	Age (Ma)	O.unive	G.cglob	G.ruber	G.tenel	G.saccu	S.dehis	G.aequi	G.calid	G.bullo	G.falco	G.digit	G.rubes	G.pac R	N.duter
1H-1, 1	0.01	0.001	0.895	4.251	21.924	0.000	15.213	0.895	5.369	1.119	5.817	0.000	0.000	0.000	0.000	16.107
1H-1, 11	0.11	0.006	0.619	2.474	32.165	0.412	15.876	0.000	4.124	1.856	4.948	0.000	0.412	0.000	0.000	10.516
1H-1, 21	0.21	0.010	0.781	0.312	35.156	0.156	10.625	0.000	2.969	1.406	6.562	0.156	0.000	0.000	0.000	14.844
1H-1, 31	0.31	0.015	0.138	0.688	35.488	1.651	8.253	0.000	4.539	1.651	6.190	0.138	0.138	0.000	0.000	7.978
1H-1, 41	0.41	0.019	0.840	2.353	21.344	1.849	6.387	0.336	2.185	2.017	7.227	0.000	0.168	0.000	0.000	19.328
1H-1, 51	0.51	0.024	0.325	2.602	12.520	0.325	8.130	0.163	1.789	1.951	8.130	0.325	0.000	0.325	0.000	21.463
1H-1, 61	0.61	0.029	0.723	1.627	17.722	0.000	5.244	0.181	3.978	1.085	6.691	0.723	0.181	1.266	0.000	19.349
1H-1, 71	0.71	0.034	0.369	2.214	15.498	0.000	5.166	0.185	4.981	2.029	11.255	0.185	0.738	0.000	0.000	15.314
1H-1, 81	0.81	0.038	0.731	1.316	17.251	1.316	5.702	0.000	3.070	2.339	7.310	0.146	0.439	0.439	0.000	12.865
1H-1, 91	0.91	0.043	0.883	2.297	12.544	0.177	4.594	0.000	2.120	1.237	8.127	0.177	0.530	0.353	0.000	13.604
1H-1, 101	1.01	0.048	0.303	1.061	15.909	0.758	6.364	0.151	1.364	0.909	10.909	0.151	0.000	0.758	0.000	11.667
1H-1, 111	1.11	0.053	0.955	1.274	13.057	1.274	3.822	0.637	3.185	1.274	9.236	0.318	0.000	0.637	0.000	6.688
1H-1, 121	1.21	0.058	0.476	0.714	18.809	0.952	5.000	0.000	4.762	2.619	5.714	0.238	0.952	0.476	0.000	15.000
1H-1, 131	1.31	0.063	0.829	1.303	22.512	0.356	8.768	0.356	2.133	1.540	5.450	0.118	0.474	0.237	0.118	17.417
1H-1, 141	1.41	0.067	0.439	2.339	14.328	2.339	6.140	0.146	3.316	2.778	4.971	0.146	0.439	0.731	0.000	13.012
1H-2, 1	1.51	0.071	0.484	0.000	10.896	3.632	4.601	0.484	1.453	0.484	7.748	1.453	0.242	0.726	0.000	16.707
1H-2, 11	1.61	Ash A														
1H-2, 21	1.71	Ash A														
1H-2, 31	1.81	Ash A														
1H-2, 41	1.91	0.076	0.344	1.375	9.966	1.031	6.873	1.031	1.718	1.031	5.498	0.000	0.344	0.344	0.000	14.089
1H-2, 51	2.01	Ash B														
1H-2, 61	2.11	0.079	0.225	0.899	15.506	0.449	11.461	0.449	2.697	2.022	7.191	0.449	1.124	0.000	0.000	12.809
1H-2, 71	2.21	0.080	1.571	1.745	24.084	0.349	9.424	0.524	5.236	2.269	4.188	0.349	0.873	0.000	0.000	8.551
1H-2, 81	2.31	0.089	0.536	3.393	12.321	0.893	7.500	0.357	2.679	1.250	7.500	0.893	0.179	0.000	0.000	11.250
1H-2, 91	2.41	0.099	0.000	2.321	13.036	0.893	11.964	0.714	3.393	2.143	4.821	0.000	0.357	0.357	0.179	15.179
1H-2, 101	2.51	0.107	0.536	2.681	11.528	0.000	7.775	0.804	3.217	1.341	4.021	0.000	0.804	0.000	0.000	21.716
1H-2, 111	2.61	0.114	0.509	1.019	10.526	0.340	5.603	0.000	1.528	0.849	3.396	0.170	0.509	0.340	0.170	17.997
1H-2, 121	2.71	0.122	0.000	2.832	7.407	0.871	14.379	0.654	2.832	1.089	8.932	0.000	0.000	0.436	0.000	23.094
1H-2, 131	2.81	0.126	0.338	1.239	28.604	0.338	11.599	0.113	3.716	2.027	5.969	0.338	0.113	0.113	0.000	12.838
1H-2, 141	2.91	0.131	0.976	1.301	21.626	1.626	10.894	0.000	2.114	1.951	6.667	0.650	0.163	0.163	0.163	11.057
1H-3, 1	3.01	0.135	0.529	0.741	14.180	2.434	7.302	0.212	1.587	2.116	8.783	1.164	0.212	0.212	0.000	17.778
1H-3, 11	3.11	0.142	1.024	1.536	23.550	0.341	11.263	0.341	1.877	2.560	5.631	0.512	0.341	0.341	0.171	16.553
1H-3, 21	3.21	0.149	0.879	0.977	29.199	0.977	11.621	0.098	2.930	2.051	5.664	0.195	0.098	0.391	0.000	11.035
1H-3, 31	3.31	0.157	1.844	1.928	26.152	1.676	10.897	0.168	2.012	3.185	3.604	0.168	0.252	0.252	0.000	14.585
1H-3, 41	3.41	0.164	0.446	2.232	16.518	0.893	9.821	0.223	2.009	1.339	6.250	1.339	0.223	0.893	0.446	17.411
1H-3, 51	3.51	0.171	0.629	1.048	18.868	0.839	6.499	0.000	3.354	1.677	7.338	0.210	0.000	1.048	0.419	19.078
1H-3, 61	3.61	0.177	0.890	2.671	14.243	0.594	8.605	0.000	2.967	2.967	4.154	0.297	0.297	1.187	0.890	22.255
1H-3, 71	3.71	0.183	0.382	1.721	16.826	0.765	8.413	0.191	1.530	2.103	3.633	0.000	0.000	0.956	1.147	18.356
1H-3, 81	3.81	0.189	0.209	2.511	10.670	0.837	4.184	0.209	1.883	1.674	6.695	0.628	0.418	0.418	0.628	15.690
1H-3, 91	3.91	0.194	0.704	1.408	16.667	0.235	8.685	0.000	3.521	0.939	2.347	0.000	0.469	0.000	0.235	17.840
1H-3, 101	4.01	0.205	0.325	1.948	5.520	0.000	7.468	0.325	3.247	0.325	2.273	0.325	0.000	0.000	0.000	10.714
1H-3, 111	4.11	0.211	0.000	0.848	13.136	0.636	5.720	0.212	1.059	1.059	8.475	0.636	0.000	0.212	0.000	16.314
1H-3, 121	4.21	0.218	0.000	2.169	16.145	0.482	9.157	0.241	1.928	0.964	4.819	0.241	0.723	0.482	0.000	19.518
1H-3, 131	4.31	0.223	0.592	2.071	18.935	0.296	10.059	0.296	2.071	1.183	5.917	0.000	0.000	0.000	0.000	21.302
1H-3, 141	4.41	0.228	0.338	2.196	16.892	0.338	10.304	0.169	2.872	0.845	5.236	0.169	0.000	0.169	0.000	17.230
1H-4, 1	4.51	0.232	0.480	0.480	10.791	0.959	2.638	0.000	1.439	1.439	5.516	0.719	0.000	1.199	0.959	18.465
1H-4, 11	4.61	0.237	0.516	1.289	18.557	0.000	10.567	0.000	3.351	2.320	5.670	0.773	0.000	0.000	0.000	14.175
1H-4, 21	4.71	0.240	0.957	0.239	32.297	0.239	13.876	0.000	2.153	0.957	2.871	0.000	0.479	0.000	0.479	10.287
1H-4, 31	4.81	0.244	0.442	0.736	19.588	0.147	14.138	0.000	1.031	1.325	3.682	0.147	0.000	0.000	0.147	16.200
1H-4, 41	4.91	0.247	0.857	0.857	13.714	0.857	7.143	0.000	1.286	1.000	7.000	0.857	0.000	1.143	0.429	18.143
1H-4, 51	5.01	0.252	0.000	0.993	12.252	0.993	9.934	0.000	1.656	0.993	4.967	0.993	0.000	1.656	0.000	18.212
1H-4, 61	5.11	0.257	0.699	0.466	17.016	0.466	11.422	0.000	1.632	0.932	8.392	0.466	0.000	1.166	0.466	11.422
1H-4, 71	5.21	0.263	0.194	0.583	20.777	0.777	11.650	0.194	3.301	1.748	6.796	0.388	0.583	1.359	0.000	18.252
1H-4, 81	5.31	0.268	0.398	2.783	24.056	0.795	14.314	0.199	2.783	0.795	3.181	0.596	0.199	0.795	0.199	11.332
1H-3, 81	5.32	0.269	1.587	1.587	27.381	0.397	13.095	0.000	3.175	1.190	2.381	0.000	1.190	0.397	0.000	12.698
1H-3, 91	5.42	0.278	0.000	0.000	23.673	0.664	3.982	0.000	1.106	0.664	8.628	0.443	0.885	1.549	1.106	11.726
1H-3, 101	5.52	0.287	0.000	0.356	15.303	1.779	8.541	0.000	0.356	1.068	9.609	0.000	1.068	1.779	0.000	15.658
1H-3, 111	5.62	0.295	0.000	0.329	18.092	0.329	10.197	0.000	1.645	0.987	6.908	0.000	0.987	0.000	0.987	19.408
1H-3, 121	5.72	0.301	0.298	1.190	16.964	0.893	10.417	0.000	3.571	1.488	4.464	0.000	0.298	0.000	0.298	11.309
1H-3, 131	5.82	0.306	1.094	0.000	17.068	2.188	7.221	0.000	1.750	0.000	10.722	0.875	0.219	0.438	0.000	12.910
1H-3, 141	5.92	0.311	0.932	0.699	12.121	0.466	2.797	0.000	2.564	0.466	9.557	0.233	0.466	0.932	0.000	17.716
1H-4, 1	6.02	0.316	1.556	1.167	11.673	1.167	5.058	0.000	3.113	2.335	7.004	0.000	0.389	0.389	0.000	19.844
1H-4, 11	6.12	0.321	2.333	1.333	12.333	0.000	10.333	0.000	3.667	0.667	5.000	0.000	0.000	0.000	0.333	18.000
1H-4, 21	6.22	0.326	1.678	1.007	10.067	0.336	4.027	0.336	1.342	1.342	5.705	0.000	0.336	0.336	0.336	11.745
1H-4, 31	6.32	0.331	1.181	0.394	17.323	0.000	11.417	0.394	4.331	2.756	3.150	0.000	0.394	0.000	0.000	21.260
1H-4, 41	6.42	0.334	0.959	0.719	33.573	0.240	14.868	0.240	4.077	1.679	3.597	0.000	0.000	0.000	0.000	11.511
1H-4, 51	6.52	0.338	1.399	0.233	35.198	1.166	13.986	0.000	4.895	1.632	3.730	0.000	0.233	0.233	0.000	10.723
1H-4, 61	6.62	0.341	2.344	0.391	18.359	3.125	7.812	0.391	1.953	2.344	2.344	1.562	0.391	0.781	0.000	14.844
1H-4, 71	6.72	0.349	0.926	0.463	15.278	3.241	5.093	0.000	3.241	2.315	8.333	1.852	0.926	1.389	0.000	15.741
1H-4, 81	6.82	0.357	1.412	0.706	21.882	0.471	8.235	0.000	3.059	2.118	2.824	0.941	1.177	0.235	0.000	17.647
1H-4, 91	6.92	0.365	1.681	0.840	18.067	0.000	9.244	0.000	2.521	0.840	3.361	0.840	0.000	0.000	0.000	14.706
1H-4, 101	7.02	0.373	0.692	1.038	20.069	0.000	5.882	0.346	1.730	0.692	7.266	1.038	0.692	1.384	0.000	11.419
1H-4, 111	7.12	0.381	1.152	1.152	22.811	0.691	8.064	0.461	3.226	0.922	2.995	0.000	0.461	0.230	0.000	11.060
1H-4, 121	7.22	0.388	1.026	0.513	23.846	0.256	8.205	0.256	3.333	1.026	4.359	0.513	0.513	0.000	0.000	14.103
1H-4, 131	7.32	0.396	0.418	0.418	6.695	0.000	5.858	2.092	3.766	2.511	1.255	0.000	1.255	0.000	0.000	15.900
1H-4, 141	7.42	0.404	0.000	0.518	12.435	2.591	5.181	1.036	2.591	1.036	5.181	0.000	1.036	0.518	0.000	10.881
2H-1, 1	7.43	0.405	1.506	0.301	17.470	0.000	9.337	1.205	3.916	1.506	4.518	0.000	0.904	0.301	0.000	13.554
2H-1, 11	7.53	0.419	0.781	2.734	10.928	0.000	15.234	0.781	5.469	2.734	4.297	0.000	0.391	0.000	0.000	13.281
2H-1, 21	7.63	0.434	1.282	2.564	21.154	2.137	11.752	0.427	2.992	1.496	5.128	0.855	0.214	0.214	0.000	18.376
2H-1, 31	7.73	0.443	1.724	2.874	19.157	1.149	13.218	0.383	2.874	1.916	2.874	0.575	0.383	0.766	0.000	12.835
2H-1, 41	7.83	0.452	1.695	0.726	19.855	1.211	12.107	0.000	4.116	1.453	3.874	0.242	0.000	0.484	0.000	14.044
2H-1, 51	7.93	0.460	1.029	1.323	21.618	1.471	7.500	0.000	3.382	1.323	7.353	0.294	0.441	0.882	0.147	18.235
2H-1, 61	8.03	0.469	0.612	1.835	18.349	0.306	9.480	0.306	2.141	2.141	3.364	0.000	1.223	0.000	0.306	17.431
2H-1, 71	8.13	0.478	1.025	2.459	14.754	1.025	13.525	0.205	1.025	2.049	2.869	0.000	0.410	0.205	0.000	14.549
2H-1, 81	8.23	0.491	0.533	0.000	16.800	2.400	2.400	1.333	3.200	0.533	4.533	0.000	0.523	0.000	0.000	10.933
2H-1, 91	8.33	0.513	1.345	1.345	3.139	0.000	3.139	0.897	2.691	0.897	3.587	0.000	0.000	0.000	0.000	13.453
2H-1, 101	8.43	0.525	0.000	0.000	7.407	0.463	8.333	0.926	2.778	0.926	2.778	0.463	1.852	0.000	0.463	17.130
2H-1, 111	8.53	Ash C														
2H-1, 121	8.63	0.538	2.051	0.000	6.667	0.000	5.641	0.000	3.590	0.513	0.513	0.000	0.513	0.000	0.000	16.410
2H-1, 131	8.73	0.552	0.943	0.943	12.264	4.717	5.975	1.258	2.516	1.572	7.233	0.629	0.000	0.629	0.315	14.465
2H-1, 141	8.83	0.556	1.303	2.606	16.287	0.000	15.309	0.651	4.560	1.954	4.560	0.651	0.651	0.326	0.000	11.075
2H-2, 1	8.93	0.559	1.194	0.000	20.597	0.896	8.060	0.896	1.791	0.299	5.373	0.299	0.597	0.000	0.000	10.448

Table 1 (continued).

Core, section Interval (cm)	Composite depth(m)	Age (Ma)	G.cglom	G.hexag	P.obliq	G.infla	G.trn L	G.trn R	G.crasf	P-D int	G.hirsu	G.scitu	G.menar	G.tumid	G.gluti
1H-1, 1	0.01	0.001	4.698	1.119	9.620	0.000	0.000	0.000	0.000	0.447	0.000	0.000	7.830	0.671	4.027
1H-1, 11	0.11	0.006	3.711	2.474	7.835	0.000	0.000	0.000	0.000	0.206	0.000	0.206	3.711	0.000	8.454
1H-1, 21	0.21	0.010	1.875	2.031	7.188	0.000	0.000	0.000	0.156	0.000	0.312	0.469	2.969	0.000	12.031
1H-1, 131	0.31	0.015	0.688	3.439	8.253	0.000	0.000	0.000	0.000	0.138	0.000	0.550	3.164	0.138	16.781
1H-1, 41	0.41	0.019	2.857	1.681	12.437	0.000	0.000	0.000	1.008	0.840	0.000	0.168	6.555	0.504	9.916
1H-1, 51	0.51	0.024	2.114	1.9S1	13.333	0.000	0.000	0.000	0.813	1.138	0.325	0.163	9.756	1.626	10.732
1H-1, 61	0.61	0.029	3.255	1.989	11.754	0.000	0.000	0.000	0.181	0.723	0.542	0.000	11.935	0.904	9.946
1H-1, 71	0.71	0.034	6.273	1.107	18.819	0.000	0.000	0.000	0.553	0.185	0.000	0.000	10.517	1.107	3.505
1H-1, 81	0.81	0.038	4.386	1.901	19.591	0.000	0.000	0.000	0.877	0.585	0.292	0.146	9.357	0.292	9.649
1H-1, 91	0.91	0.043	3.003	1.S90	26.855	0.000	0.000	0.000	0.883	0.530	0.530	0.177	10.424	1.S90	7.774
1H-1, 101	1.01	0.048	3.030	2.121	18.030	0.000	0.000	0.000	0.455	0.151	0.151	0.606	9.848	1.212	14.091
H-1, 111	1.11	0.053	4.140	1.274	21.338	0.000	0.000	0.000	0.000	0.000	0.637	0.000	18.790	1.911	9.554
1H-1, 121	1.21	0.058	4.524	0.476	20.476	0.000	0.000	0.000	0.238	0.714	0.476	0.000	12.143	1.190	4.048
1H-1, 131	1.31	0.063	5.569	2.014	14.100	0.000	0.000	0.000	0.237	0.237	0.592	0.000	7.346	0.356	7.938
H-1, 141	1.41	0.067	4.971	1.608	14.181	0.000	0.000	0.000	2.485	0.731	0.292	0.146	9.211	1.901	13.450
1H-2, 1	1.51	0.071	3.632	0.242	11.864	0.000	0.000	0.000	2.179	0.726	0.000	0.000	13.317	3.874	15.254
1H-2, 11	1.61	Ash A													
1H-2, 21	1.71	Ash A													
1H-2, 31	1.81	AshA													
1H-2, 41	1.91	0.076	8.591	1.031	18.557	0.000	0.000	0.000	0.687	0.000	0.000	0.000	14.777	4.467	8.247
1H-2, 51	2.01	AshB													
1H-2, 61	2.11	0.079	5.843	1.124	13.933	0.000	0.000	0.000	0.674	0.449	0.225	0.449	11.236	0.449	10.337
1H-2, 71	2.21	0.080	6.108	1.047	12.565	0.000	0.000	0.000	1.396	0.349	0.174	0.000	10.820	0.524	7.853
1H-2, 81	2.31	0.089	7.321	0.714	13.036	0.000	0.000	0.000	0.714	0.357	0.179	0.000	12.679	1.964	14.286
1H-2, 91	2.41	0.099	5.714	1.429	9.464	0.000	0.000	0.000	3.214	1.250	0.179	0.179	11.964	1.071	10.179
1H-2, 101	2.51	0.107	6.702	0.536	10.992	0.000	0.000	0.000	1.072	2.413	0.000	0.000	17.962	4.289	1.609
1H-2, 111	2.61	0.114	2.886	0.849	14.601	0.000	0.000	0.000	2.207	1.698	0.000	0.000	19.694	3.226	11.885
1H-2, 121	2.71	0.122	4.357	1.089	10.240	0.000	0.000	0.000	0.436	1.961	0.000	0.436	11.547	1.743	5.664
1H-2, 131	2.81	0.126	2.590	3.378	5.180	0.000	0.000	0.000	0.225	0.563	0.225	0.113	4.730	0.451	15.203
1H-2, 141	2.91	0.131	4.390	1.301	9.919	0.000	0.000	0.000	0.325	1.951	0.325	0.488	7.968	0.325	13.658
1H-3, 1	3.01	0.135	2.646	1.270	12.698	0.000	0.000	0.000	2.116	1.587	0.000	0.212	8.571	0.635	13.016
1H-3, 11	3.11	0.142	4.607	2.218	10.580	0.000	0.000	0.000	1.877	0.000	0.000	0.341	7.338	0.853	6.143
1H-3, 21	3.21	0.149	4.883	2.832	9.473	0.000	0.000	0.000	0.684	0.684	0.391	0.000	5.664	0.293	8.984
1H-3, 31	3.31	0.157	3.772	1.760	7.963	0.000	0.000	0.000	1.509	1.006	0.084	0.000	8.801	0.419	7.963
1H-3, 41	3.41	0.164	3.571	1.786	11.384	0.000	0.000	0.000	0.670	2.455	1.339	0.000	8.259	1.339	9.152
1H-3, 51	3.51	0.171	2.306	3.145	10.482	0.000	0.000	0.000	0.419	2.725	1.048	0.000	9.853	0.839	8.176
1H-3, 61	3.61	0.177	2.374	2.374	12.463	0.000	0.000	0.000	0.594	2.374	0.000	0.000	11.869	0.594	5.341
1H-3, 71	3.71	0.183	2.868	0.574	8.031	0.000	0.000	0.000	1.530	2.103	0.191	0.191	12.428	2.294	13.767
1H-3, 81	3.81	0.189	2.720	1.046	18.619	0.000	0.000	0.000	1.883	1.046	0.209	0.000	14.017	3.975	9.833
1H-3, 91	3.91	0.194	9.390	1.174	17.606	0.000	0.000	0.000	0.939	1.643	0.704	0.000	11.972	0.704	2.817
1H-3, 101	4.01	0.205	7.143	0.325	17.208	0.000	0.000	0.000	5.520	1.299	0.000	0.000	26.948	5.844	3.247
1H-3, 111	4.11	0.211	4.873	0.636	13.983	0.000	0.000	0.000	2.966	3.814	0.000	0.000	17.585	1.695	6.144
1H-3, 121	4.21	0.218	2.892	1.928	9.398	0.000	0.000	0.000	2.892	0.482	0.000	0.723	15.422	0.723	8.675
1H-3, 131	4.31	0.223	5.325	0.888	10.059	0.000	0.000	0.296	0.888	0.592	0.000	0.592	11.539	0.296	6.805
1H-3,141	4.41	0.228	6.081	2.027	11.318	0.000	0.000	0.338	3.378	1.520	0.169	0.169	10.473	1.013	6.757
1H-4, 1	4.51	0.232	2.398	0.959	14.628	0.000	0.000	0.000	4.077	2.638	0.000	0.240	15.588	2.638	11.751
1H-4, 11	4.61	0.237	6.701	0.773	10.567	0.000	0.000	0.000	2.062	2.062	0.258	0.000	14.949	0.258	5.155
1H-4, 21	4.71	0.240	2.632	2.153	11.244	0.000	0.000	0.000	1.435	0.479	0.957	0.000	6.220	0.239	9.809
1H-4, 31	4.81	0.244	3.240	1.325	11.782	0.000	0.000	0.000	1.767	1.473	0.295	0.000	9.131	0.589	12.813
1H-4, 41	4.91	0.247	1.571	1.143	16.714	0.000	0.000	0.000	2.286	1.286	0.000	0.000	10.857	1.000	11.857
1H-4, 51	5.01	0.252	2.318	1.324	12.914	0.000	0.000	0.000	3.311	2.980	0.000	0.331	9.934	1.324	12.914
1H-4, 61	5.11	0.257	2.564	0.233	13.054	0.000	0.000	0.000	1.399	0.233	1.166	0.000	15.851	1.865	9.091
1H-4, 71	5.21	0.263	3.883	1.359	8.544	0.000	0.000	0.000	2.136	0.777	0.000	0.194	7.379	0.583	8.544
1H-4, 81	5.31	0.268	6.561	1.392	11.133	0.000	0.000	0.000	3.579	0.994	0.000	0.199	6.561	3.976	3.181
1H-3, 81	5.32	0.269	5.556	2.381	9.127	0.397	0.000	0.000	3.175	0.397	0.397	0.000	7.143	2.381	3.968
1H-3, 91	5.42	0.278	1.549	0.664	9.292	0.000	0.000	0.000	3.097	3.097	0.000	0.443	11.504	0.885	15.044
1H-3, 101	5.52	0.287	2.847	0.356	9.609	0.000	0.000	0.000	2.847	1.779	0.356	0.000	11.744	0.712	14.235
1H-3, 111	5.62	0.295	4.276	1.645	7.566	0.000	0.000	0.000	3.290	3.290	0.000	0.658	17.105	0.000	2.303
1H-3, 121	5.72	0.301	6.250	2.083	15.179	0.000	0.000	0.000	2.381	1A88	0.000	0.298	13.988	1.786	5.357
1H-3, 131	5.82	0.306	2.845	0.656	9.847	0.000	0.000	0.000	3.063	3.063	0.219	0.000	11.379	0.875	13.567
1H-3, 141	5.92	0.311	2.564	0.466	11.422	0.000	0.000	0.000	1.865	2.564	0.000	0.000	17.016	4.662	10.490
1H-4, 1	6.02	0.316	3.891	0.778	14.397	0.000	0.000	0.000	0.778	0.778	0.000	0.000	18.288	2.335	5.058
1H-4, 11	6.12	0.321	9.333	1.000	16.333	0.000	0.000	0.000	1.000	0.000	0.333	0.333	13.333	1.667	2.667
1H-4, 21	6.22	0.326	3.020	0.000	20.470	0.000	0.000	0.000	2.685	1.678	0.000	0.000	17.450	4.027	12.080
1H4, 31	6.32	0.331	5.905	2.362	11.024	0.000	0.000	0.000	0.394	1.181	0.000	0.000	9.842	2.756	3.937
1H4, 41	6.42	0.334	4.077	4.316	5.516	0.000	0.000	0.000	0.719	0.000	0.959	0.240	3.118	0.000	9.592
1H4, 51	6.52	0.338	3.730	1.865	5.361	0.000	0.000	0.000	0.000	0.000	0.000	0.233	3.030	0.233	12.121
1H4, 61	6.62	0.341	1.172	0.000	9.375	0.000	0.000	0.000	1.953	1.953	0.000	0.000	14.453	1.953	12.500
1H4, 71	6.72	0.349	1.852	0.926	10.185	0.000	0.000	0.000	2.315	0.463	0.926	0.000	11.574	1.38S	11.574
1H4, 81	6.82	0.357	1.412	3.059	12.235	0.000	0.000	0.000	0.706	2.118	0.000	0.000	10.353	0.471	8.941
1H4, 91	6.92	0.365	8.824	1.681	14.706	0.000	0.000	0.000	0.840	0.840	0.000	0.000	15.546	1.681	3.782
1H-4, 101	7.02	0.373	4.844	0.692	19.723	0.000	0.000	0.000	0.692	0.346	0.000	0.000	13.495	1.384	6.574
1H4, 111	7.12	0.381	3.456	1.152	18.664	0.000	0.000	0.000	0.922	0.230	0.230	0.000	12.903	1.152	8.064
1H4, 121	7.22	0.388	3.846	0.000	14.615	0.000	0.000	0.000	0.513	0.000	0.000	0.513	15.641	1.282	5.641
1H4, 131	7.32	0.396	0.837	0.418	18.410	0.000	0.000	0.000	0.837	2.092	0.000	0.000	25.523	9.623	2.092
1H4, 141	7.42	0.404	1.554	1.036	15.026	0.000	0.000	0.000	0.000	0.518	0.000	0.000	17.098	9.845	11.917
2H-1, 1	7.43	0.405	4.518	1.506	15.964	0.000	0.000	0.000	1.807	0.000	0.000	0.301	13.253	4.819	3.313
2H-1, 11	7.53	0.419	6.641	0.391	13.281	0.000	0.000	0.000	1.562	1.953	0.000	0.000	12.109	4.688	2.734
2H-1, 21	7.63	0.434	3.205	1.068	8.333	0.000	0.000	0.000	1.282	0.641	0.000	0.000	6.624	1.923	8.333
2H-1, 31	7.73	0.443	4.406	1.341	12.835	0.000	0.000	0.000	0.575	0.383	0.000	0.000	10.153	1.916	7.663
2H-1, 41	7.83	0.452	3.874	1.453	14.286	0.000	0.000	0.000	0.484	0.726	0.000	0.000	7.748	2.906	8.717
2H-1, 1	7.93	0.460	2.794	1.323	9.853	0.147	0.000	0.000	0.441	1.029	0.000	0.000	8.382	2.500	8.529
2H-1, 61	8.03	0.469	5.199	0.917	14.373	0.000	0.000	0.000	1.223	1.529	0.000	0.000	10.092	2.141	7.034
2H-1, 71	8.13	0.478	3.074	0.820	16.598	0.000	0.000	0.000	1.434	0.000	0.000	0.000	10.041	3.688	10.246
2H-1, 81	8.23	0.491	2.667	0.533	20.533	0.000	0.000	0.267	1.333	0.000	0.000	0.000	10.667	5.067	15.733
2H-1, 91	8.33	0.513	1.345	0.897	33.632	0.000	0.000	0.000	0.897	0.448	0.000	0.448	18.834	9.865	3.139
2H-1, 101	8.43	0.525	2.778	0.000	30.093	0.000	0.000	0.000	0.000	2.778	0.000	0.463	7.407	9.722	3.241
2H-1, 111	8.53	Ash C													
2H-1, 121	8.63	0.538	1.539	0.000	38.461	0.000	0.000	0.000	0.513	0.000	0.000	0.000	11.795	9.744	2.051
2H-1, 131	8.73	0.552	2.201	0.629	21.384	0.000	0.000	0.000	0.000	0.315	0.000	0.315	7.233	4.402	10.063
2H-1, 141	8.83	0.556	2.280	0.977	22.476	0.000	0.000	0.000	0.977	0.000	0.000	0.000	7.818	1.954	3.583
2H-2, 1	8.93	0.559	2.388	2.687	22.388	0.000	0.000	0.896	1.194	0.000	0.000	0.299	7.761	3.582	8.358

Table 1 (continued).

Core, section interval (cm)	Composite depth (m)	Age (Ma)	O.unive	G.cglob	G.ruber	G.tenel	G.saccu	S.dehis	G.aequi	G.calid	G.bullo	G.falco	G.digit	G.rubes	G.pac R	N.duter
2H-2, 11	9.03	0.563	1.592	0.531	25.995	4.244	5.570	0.531	1.592	2.387	4.244	0.531	0.000	1.592	0.000	14.058
2H-2, 21	9.13	0.566	0.552	0.735	17.647	3.125	7.169	0.184	2.206	1.471	4.412	0.368	0.184	0.368	0.184	21.324
2H-2, 31	9.23	0.569	0.662	0.331	7.616	0.000	8.278	2.318	5.960	0.662	3.311	0.000	0.331	0.000	0.000	26.159
2H-2, 41	9.33	0.572	0.000	0.796	5.570	0.000	6.897	1.326	4.244	0.531	3.448	0.265	0.796	0.000	0.531	16.976
2H-2, 51	9.43	0.576	0.926	2.315	4.630	0.000	11.111	1.620	4.398	3.241	9.491	0.694	1.157	0.000	0.000	14.120
2H-2, 61	9.53	0.581	1.527	2.290	9.733	0.000	8.206	0.763	3.244	1.908	11.832	0.763	1.336	0.000	0.000	17.939
2H-2, 71	9.63	0.585	0.510	0.510	11.395	1.361	5.442	0.510	1.701	1.020	7.993	0.510	0.170	0.000	0.000	15.986
2H-2, 81	9.73	0.590	0.370	0.741	13.333	3.148	7.407	0.741	2.037	2.222	8.333	0.741	0.185	0.185	0.000	23.704
2H-2, 91	9.83	0.596	0.397	0.397	10.714	0.397	7.540	1.587	1.984	1.190	9.921	0.000	0.794	0.000	0.000	14.286
2H-2, 101	9.93	0.607	1.132	0.755	5.283	0.000	10.189	1.887	3.774	2.642	7.925	1.132	0.755	0.000	0.000	13.585
2H-2, 111	10.03	0.617	1.136	0.568	16.477	1.420	12.216	1.136	2.841	2.841	11.080	0.568	0.568	0.000	0.000	15.909
2H-2, 121	10.13	0.623	0.388	0.194	24.272	1.942	11.262	0.388	2.524	2.718	6.408	0.777	0.388	0.000	0.000	12.039
2H-2, 131	10.23	0.628	0.379	1.705	11.932	2.462	10.606	0.568	2.273	1.894	7.954	1.894	0.568	0.000	0.000	17.803
2H-2, 141	10.33	0.634	0.675	1.180	16.695	3.879	12.648	0.675	2.698	1.180	10.287	1.349	0.337	0.169	0.000	11.973
2H-3, 1	10.43	0.641	0.534	1.957	12.989	3.203	8.541	0.534	3.203	2.313	9.075	1.246	0.712	0.178	0.178	16.726
2H-3, 11	10.53	0.648	0.137	0.956	16.120	3.552	9.699	0.410	2.049	1.776	5.601	0.546	0.410	0.137	0.000	15.164
2H-3, 21	10.63	0.655	0.571	0.000	14.857	3.429	7.429	0.571	3.429	5.143	8.000	0.000	1.714	0.000	0.000	12.000
2H-3, 31	10.73	0.662	1.185	3.317	22.986	2.133	7.109	1.185	3.081	1.422	3.555	0.948	0.711	0.474	0.000	12.322
2H-3, 41	10.83	0.669	0.229	6.179	16.476	0.000	8.009	1.602	1.831	1.144	5.263	0.458	1.373	0.000	0.000	15.103
2H-3, 51	10.93	0.676	0.699	0.233	11.422	1.865	5.128	0.932	2.331	0.699	7.925	2.331	0.233	0.233	0.000	18.415
2H-3, 61	11.03	0.682	0.390	1.365	23.002	0.000	10.526	1.170	4.873	2.729	8.187	0.390	1.365	0.000	0.000	14.425
2H-3, 71	11.13	0.687	0.617	0.772	31.944	1.080	10.803	0.309	2.469	0.463	6.327	0.309	0.000	0.000	0.000	10.648
2H-3, 81	11.23	0.692	1.260	1.102	27.402	0.945	12.283	0.630	3.622	1.260	7.402	0.158	0.000	0.000	0.000	8.819
2H-3, 91	11.33	9.697	1.135	1.844	27.801	0.709	11.064	0.567	5.532	2.270	7.376	0.851	0.142	0.142	0.000	10.922
2H-3, 101	11.43	0.703	0.649	1.297	21.790	1.686	7.523	1.167	2.464	1.297	5.966	0.649	0.259	1.297	0.000	15.564
2H-3, 111	11.53	0.708	1.923	1.224	23.951	1.224	7.343	0.525	2.448	2.797	6.119	1.224	0.175	2.622	0.000	10.140
2H-3, 121	11.63	0.714	0.978	1.075	30.596	0.195	10.068	1.564	2.150	0.978	8.700	0.782	0.000	0.195	0.000	8.993
2H-3, 131	11.73	0.719	1.125	0.643	26.367	1.125	10.289	0.482	4.341	1.125	6.109	0.482	0.161	1.125	0.000	10.289
2H-3, 141	11.83	0.723	2.817	0.939	23.474	1.643	7.512	0.469	3.286	0.939	7.277	0.469	0.235	2.113	0.235	8.685
2H-4, 1	11.93	0.727	1.961	1.765	18.627	0.784	9.608	1.177	4.118	1.765	11.373	0.980	0.196	0.196	0.000	10.000
2H-4, 11	12.03	0.731	2.179	0.871	34.858	0.218	8.932	2.179	2.614	0.871	3.922	0.218	0.218	0.000	0.000	10.893
2H-4, 21	12.13	0.734	1.013	2.703	22.973	0.000	13.514	2.196	4.730	0.845	8.784	0.845	0.676	0.000	0.000	10.304
2H-4, 31	12.23	Ash D														
2H-4, 41	12.33	Ash D														
2H-4, 51	12.43	0.745	1.760	0.550	32.673	1.320	14.081	0.440	2.640	1.430	4.180	0.440	0.000	0.000	0.000	7.481
2H-4, 61	12.53	0.748	1.560	1.404	30.889	1.248	13.729	0.780	2.652	2.184	5.148	0.624	0.312	0.936	0.000	7.488
2H-4, 71	12.63	0.752	0.718	1.196	21.770	1.196	19.139	0.000	2.632	1.196	5.742	0.718	0.239	0.957	0.000	6.938
2H-4, 81	12.73	0.756	1.367	0.456	15.490	1.139	13.212	0.456	1.367	2.506	12.301	1.594	0.911	0.000	0.228	5.923
2H-4, 91	12.83	0.760	0.540	0.899	20.683	0.180	10.432	0.899	1.799	1.799	9.712	0.899	1.079	0.000	0.000	12.230
2H-4, 101	12.93	0.765	0.641	2.350	14.744	0.000	11.111	1.496	1.496	1.496	9.829	1.923	1.068	0.427	0.000	8.333
2H-4, 111	13.03	0.769	0.895	1.610	28.086	0.000	10.018	1.968	0.895	2.147	9.123	0.358	0.716	0.358	0.000	9.302
2H-4, 121	13.13	0.773	0.844	2.954	18.143	0.000	8.650	1.266	1.477	0.422	8.439	0.211	0.000	0.211	0.211	11.392
2H-4, 131	13.23	0.777	0.500	0.250	16.750	0.000	8.250	1.500	1.250	1.250	7.750	1.000	0.000	0.500	0.000	16.250
2H-4, 141	13.33	0.782	0.484	0.969	16.465	0.242	8.959	2.421	2.421	1.695	7.990	0.000	0.000	0.000	0.000	10.170
2H-5, 1	13.43	0.786	0.773	1.237	19.938	0.155	9.737	1.237	2.627	1.546	7.728	0.309	0.000	0.464	0.000	12.210
2H-5, 11	13.53	0.790	0.220	0.440	28.634	0.000	9.692	1.542	1.101	0.220	7.930	0.440	0.440	0.440	0.220	7.709
2H-5, 21	13.63	0.795	0.000	1.444	20.397	0.542	4.874	1.083	0.722	0.902	8.484	0.902	0.181	1.625	0.181	17.274
2H-5, 31	13.73	0.799	0.733	0.293	19.501	1.026	7.478	1.906	1.026	1.026	8.211	0.147	0.147	1.466	0.000	13.343
2H-5, 41	13.83	0.806	0.969	1.453	25.666	0.242	10.412	0.969	2.179	1.937	8.717	0.726	0.000	0.726	0.000	6.053

FL appears to have deepened below the depth of Site 758 during the $\delta^{18}O$ stages 20, 18, and 6 and during the glacial to interglacial transitions from $\delta^{18}O$ stages 18 to 17, 16 to 15, 10 to 9, 8 to 7, 6 to 5, and 2 to 1.

The relationship among RSP%, coarse fraction, and $\delta^{18}O$ is generally characterized by low coarse fraction values and high RSP% during interglacial stages and high coarse fraction values and low RSP% during glacials (Fig. 3). The quasi-periodic 100-k.y. cycles of the late Quaternary are superimposed on a long-term dissolution cycle. The mid-point of this cycle is between 400 and 550 ka, where dissolution is greatest as indicated by the highest values of RSP% (80%) and by the lowest coarse fraction values. The coarse fraction value of 1.89% at 510 ka (Sample 121-758A-2H-1, 101 cm) is the lowest value of the past 2.9 Ma (Farrell and Janecek, this volume). At the mid-point of the cycle, the increase in the abundances of the dissolution resistant species *P. obliquiloculata*, *G. menardii*, and *G. tumida* is mirrored by the decreased abundances of the dissolution susceptible species *G. ruber*, *G. sacculifer*, *G. bulloides*, and *G. glutinata*. The dissolution trend is clearly observed in the downcore record of *G. tumida* abundance (Fig. 2). At the beginning and end of the cycle, near 25 and 750 ka, enhanced $CaCO_3$ preservation is indicated by high coarse fraction values and low RSP%.

DISCUSSION

Effects of Dissolution on Faunal Assemblages

The relative abundance of planktonic foraminifers distributed on the seafloor is largely determined by the carbonate chemistry of the waters bathing the foraminifers. $CaCO_3$ dissolution determines which species will be preserved in the fossil assemblage (Bé and Hutson, 1977; Cullen and Prell, 1984). We document variations in $CaCO_3$ preservation based on faunal variations, faunal dissolution indices, and coarse fraction. The relationships between the coarse fraction values of each sample (a proxy for dissolution) and the abundances of eight major foraminifer species in the same sample are shown in Figure 5. The trends show that high coarse fraction is generally associated with high percentages of dissolution-susceptible species *G. ruber*, *G. sacculifer*, *G. bulloides*, and *G. glutinata*. Likewise, low coarse fraction is associated with high percentages of dissolution-resistant species *N. dutertrei*, *G. menardii*, *P. obliquiloculata*, and *G. tumida*. Good preservation is generally characterized by high abundances of the dissolution-susceptible species and high coarse fractions. Poor preservation is marked by high abundances of the dissolution-resistant species and low coarse fractions. The scatter about the trends is most likely related to a variety of ecological and/or non-preservational factors. Variations of $\%CaCO_3$ at Site 758 primarily reflect dilution by terrigenous sediments and are therefore not a reliable index of dissolution (Farrell and Janecek, this volume).

The downcore pattern of dissolution occurs at a quasi-periodic cycle of ~100 k.y., closely linked to the glacial-interglacial climatic record interpreted from the $\delta^{18}O$ to interglacials. These intervals are associated with the lowest RSP% and the highest coarse fractions.

The atypical faunal composition observed between 490 and 550 ka is attributed to a dramatic increase in $CaCO_3$ dissolution

Table 1 (continued).

Core, section Interval (cm)	Composite depth(m)	Age (Ma)	G.cglom	G.hexag	P.obliq	G.infla	G.trn L	G.trn R	G.crasf	P-D int	G.hirsu	G.scitu	G.menar	G.tumid	G.gluti
2H-2, 111	9.03	0.563	0.000	1.592	13.263	0.000	0.000	0.531	0.265	0.531	0.000	0.531	6.631	2.918	10.875
2H-2, 121	9.13	0.566	0.919	0.552	11.397	0.000	0.000	1.471	1.103	0.000	0.000	0.184	7.537	4.963	11.949
2H-2, 131	9.23	0.569	0.993	0.662	21.523	0.000	0.000	0.993	1.324	0.331	0.000	0.000	12.252	5.629	0.662
2H-2, 41	9.33	0.572	0.796	1.061	29.973	0.000	0.000	1.592	0.796	0.265	0.000	0.000	14.324	5.836	3.979
2H-2, 51	9.43	0.576	1.852	1.157	27.315	0.000	0.000	0.926	0.463	0.000	0.000	0.000	9.954	2.546	2.083
2H-2, 61	9 53	0.581	1.336	0.763	22.328	0.000	0.000	0.573	1.145	0.191	0.000	0.000	7.443	4.008	2.672
2H-2, 71	9.63	0.585	0.680	0.000	21.939	0.000	0.000	5.102	0.000	0.340	0.000	0.000	6.803	3.912	14.116
2H-2, 81	9.73	0.590	1.111	0.185	12.407	0.000	0.000	1.296	0.185	0.185	0.000	0.000	7.778	3.889	9.815
2H-2, 91	9.83	0.596	2.778	2.381	17.857	0.000	0.000	0.794	2.381	0.000	0.000	0.000	16.270	3.571	4.762
2H-2, 101	9.93	0.607	0.377	1.132	20.755	0.000	0.000	1.887	1.887	0.000	0.000	0.000	16.981	4.151	3.774
2H-2, 111	10.03	0.617	1.989	1.989	9.375	0.000	0.000	0.284	0.284	0.000	0.000	0.568	5.682	1.136	11.932
2H-2, 121	10.13	0.623	1.553	1.942	8.544	0.000	0.000	1.359	0.000	0.000	0.000	0.000	4.466	1.165	17.670
2H-2, 131	10.23	0.628	0.189	1.705	11.742	0.189	0.000	1.136	0.379	0.189	0.000	0.379	12.500	0.758	10.795
2H-2, 141	10.33	0.634	2.024	0.675	12.816	0.169	0.000	1.180	0.506	0.000	0.000	0.169	8.600	1.855	8.263
2H-3, 1	10.43	0.641	2.313	1.246	13.345	0.178	0.000	1.246	0.534	0.178	0.000	0.000	7.829	0.890	10.854
2H-3, 11	10.53	0.648	2.049	1.503	20.628	0.000	0.000	0.683	0.546	0.137	0.000	0.273	6.967	0.820	9.836
2H-3, 21	10.63	0.655	1.714	0.000	17.143	0.000	0.000	1.143	0.000	0.000	0.000	0.000	8.000	4.000	10.857
2H-3, 31	10.73	0.662	2.370	0.948	8.768	0.000	0.000	0.711	1.896	0.000	0.000	0.237	12.322	1.422	10.900
2H-3, 41	10.83	0.669	1.602	0.915	15.561	0.000	0.229	1.144	1.373	0.000	0.000	0.000	11.899	1.144	8.467
2H-3, 51	10.93	0.676	0.699	0.000	16.084	0.000	0.000	1.166	0.000	0.000	0.000	0.000	11.655	2.098	15.851
2H-3, 61	11.03	0.682	2.729	1.170	13.645	0.000	0.000	0.195	0.390	0.000	0.000	0.000	7.602	0.585	5.263
2H-3, 71	11.13	0.687	3.549	0.772	9.877	0.000	0.000	0.000	0.154	0.154	0.000	0.154	8.179	0.617	10.803
2H-3, 81	11.23	0.692	2.362	1.890	14.173	0.000	0.000	0.158	0.158	0.158	0.000	0.158	7.559	0.315	8.189
2H-3, 91	11.33	0.697	2.270	2.553	13.050	0.000	0.000	0.567	0.709	0.425	0.000	0.000	5.248	0.425	4.397
2H-3, 101	11.43	0.703	0.908	0.519	14.656	0.000	0.000	1.038	0.000	0.389	0.000	0.000	9.728	1.g46	9.209
2H-3, 111	11.53	0.708	0.874	1.748	1S.909	0.000	0.000	0.874	0.175	0.175	0.000	0.175	10.140	0.874	7.343
2H-3, 121	11.63	0.714	3.617	1.466	10.948	0.000	0.000	0.195	0.000	0.195	0.000	0.000	5.767	0.978	10.557
2H-3, 131	11.73	0.719	0.321	1.929	8.682	0.000	0.000	0.643	0.000	0.321	0.161	0.321	6.752	0.804	16.399
2H-3, 141	11.83	0.723	1.408	0.939	18.075	0.000	0.000	1.643	0.235	0.469	0.000	0.235	10.094	0.939	5.868
2H-4, 1	11.93	0.727	1.373	0.588	13.333	0.000	0.000	0.784	0.000	0.196	0.000	0.392	13.725	0.980	6.078
2H-4, 11	12.03	0.731	1.961	0.000	10.893	0.000	0.218	0.871	0.436	0.000	0.000	0.218	9.368	1.961	6.100
2H-4, 21	12.13	0.734	1.689	2.027	16.216	0.000	0.000	0.000	0.169	0.000	0.000	0.000	6.926	2.027	2.365
2H-4, 31	12.23	Ash D													
2H-4, 41	12.33	Ash D													
2H-4, 51	12.43	0.745	0.440	4.730	7.701	0.000	0.000	0.000	0.110	0.220	0.000	0.000	1.540	0.440	17.822
2H-4, 61	12.53	0.748	0.936	3.432	8.112	0.000	0.000	0.156	0.000	0.000	0.000	0.000	2.652	0.780	14.977
2H-4, 71	12.63	0.752	0.479	1.914	16.986	0.000	0.239	0.957	0.239	0.239	0.000	0.000	8.373	0.479	7.655
2H-4, 81	12.73	0.756	0.000	2.278	21.640	0.228	0.000	0.456	1.367	0.000	0.000	0.456	10.934	1.367	4.328
2H4, 91	12.83	0.760	0.000	2.338	19.065	0.000	0.000	2.158	0.180	0.000	0.000	0.540	8.633	0.719	5.216
2H-4,101	12.93	0.765	0.641	1.496	26.068	0.000	0.000	0.641	0.000	0.000	0.000	0.000	9.615	1.923	4.701
2H-4, 111	13.03	0.769	0.537	2.683	18.962	0.000	0.000	0.000	0.000	0.179	0.000	0.000	5.188	0.716	6.261
2H-4, 121	13.13	0.773	1.266	1.477	19.198	0.000	0.000	1.055	0.000	0.000	0.000	0.211	10.549	1.266	10.760
2H-4, 131	13.23	0.777	1.000	0.750	18.500	0.000	0.000	0.250	0.000	0.000	0.000	0.000	11.000	0.750	12.500
2H-4, 141	13.33	0.782	2.906	2.421	23.487	0.000	0.000	0.484	0.000	0.000	0.000	0.000	6.295	0.969	11.622
2H-5, 1	13.43	0.786	0.927	1.700	15.765	0.000	0.000	0.000	0.000	0.000	0.155	0.000	12.210	1.237	10.046
2H-5, 11	13.53	0.790	3.304	2.643	13.877	0.000	0.000	1.542	0.220	0.220	0.220	0.000	4.405	1.542	12.996
2H-5, 21	13.63	0.795	2.527	1.083	13.718	0.000	0.000	6.318	0.361	0.181	0.000	0.181	7.040	1.263	13.718
2H-5, 31	13.73	0.799	1.906	1.173	21.701	0.000	0.000	0.587	0.147	0.000	0.293	0.147	6.305	1.320	10.117
2H-5, 41	13.83	0.806	2.906	2.663	17.918	0.000	0.000	0.000	0.484	0.000	0.000	0.000	3.874	1.937	10.170

Table 2. Codes and descriptive statistics for planktonic foraminifer percentage data from Site 758 and from modern Indian Ocean sediments.

		0-800 ka at Site 758				Modern surface sediments (Prell, 1985)			
Foraminifer species	Code	Average	St. Dev.	Minimum	Maximum	Average	St. Dev.	Minimum	Maximum
Orbulina universa	O.unive	0.8172	0.5673	0.0000	2.8169	0.5680	0.7550	0.0000	4.7035
Globigernoides conglobatus	G.cglob	1.2957	0.9646	0.0000	6.1785	1.1826	1.4198	0.0000	8.1340
Globigerinoides ruber	Gruber	18.3111	7.1216	3.1390	35.4883	16.7304	13.3172	0.0000	57.9832
Globigerinoides tenellus	G.tenel	0.9507	1.0293	0.0000	4.7170	0.7683	1.1213	0.0000	7.7128
Globigerinoides sacculifer	G.saccu	9.0541	3.1658	2.4000	19.1387	7.0198	5.8355	0.0000	24.7934
Sphaeroidinella dehiscens	S.dehis	0.5667	0.5999	0.0000	2.4213	0.3052	0.6668	0.0000	5.6225
Globigerinella aequilateralis	G.aequi	2.7479	1.1404	0.3559	5.9603	2.6528	2.1633	0.0000	9.1922
Globigerina calida	G.calid	1.5496	0.7648	0.0000	5.1429	1.4470	1.4611	0.0000	9.1954
Globigerina bulloides	G.bullo	6.2646	2.4325	0.5128	12.3007	14.7020	15.8717	0.2985	67.7711
Globigerina falconensis	G.falco	0.4703	0.4771	0.0000	2.3310	1.6076	2.9509	0.0000	19.7183
Globigerina digitata	G.digit	0.4159	0.4081	0.00C0	1.851g	0.5673	1.1436	0.0000	12.7701
Globigerina rubescens	G rubes	0.4113	0.5216	0.0000	2.6224	0.6422	1.0163	0.0000	5.2817
Globigerina pachyderma R.	G.pac R	0.1008	0.2258	0.0000	1.1472	2.0782	6.7909	0.0000	71.4286
Neogloboquadrina dutertrei	N.duter	14.2684	3.9749	5.9226	26.1589	8.3539	6.9110	0.0000	35.1563
Globoquadrina conglormerata	G.cglom	3.0841	2.0242	0.0000	9.3897	1.3604	2.2379	0.0000	12.9114
Globoquadrina hexagona	G.hexag	1.3808	0.8873	0.0000	4.7305	1.0703	1.3389	0.0000	7.9625
Pulleniatina obliquiloculata	P.obliq	14.7275	5.6887	5.1802	38.4615	3.6086	3.7212	0.0000	20.7792
Globorotalia inflata	G.infla	0.0098	0.0484	0.0000	0.3968	7.1221	15.1551	0.0000	83.6420
Globorotalia truncatulinoides L.	G.trn L	0.0051	0.0339	0.0000	0.2392	1.2189	2.6638	0.0000	13.1313
Globorotalia truncatulinoides R.	G.trn R	0.3626	0.8224	0.0000	6.3177	0.4359	1.3529	0.0000	10.5802
Globorotalia crassaformis	G.crasf	1.0398	1.0599	0.0000	5.5195	0.1480	0.4565	0.0000	4.3902
"P-D intergrade"	P-D.int	0-7324	0.8934	0.0000	3.8136	1.6565	6.0487	0.0000	83.3333
Globorotalia hirsuta	G.hirsu	0.1233	0.2557	0.0000	1.3393	0.2298	0.6540	0.0000	4.4369
Globorotalia scitula	G.scitu	0.1310	0.1863	0.0000	0.7229	0.3476	0.5476	0.0000	4.6332
Globorotalia menardii	G.menar	10.4066	4.3356	1.5402	26.9480	10.0006	12.3993	0.0000	65.8192
Globorotalia tumida	G.tumid	2.0571	2.0668	0.0000	9.8655	1.2848	3.0309	0.0000	23.4657
Globigerinita glutinata	G.gluti	8.7150	3.9905	0.6623	17.8218	12.8898	10.4878	0.0000	41.6667

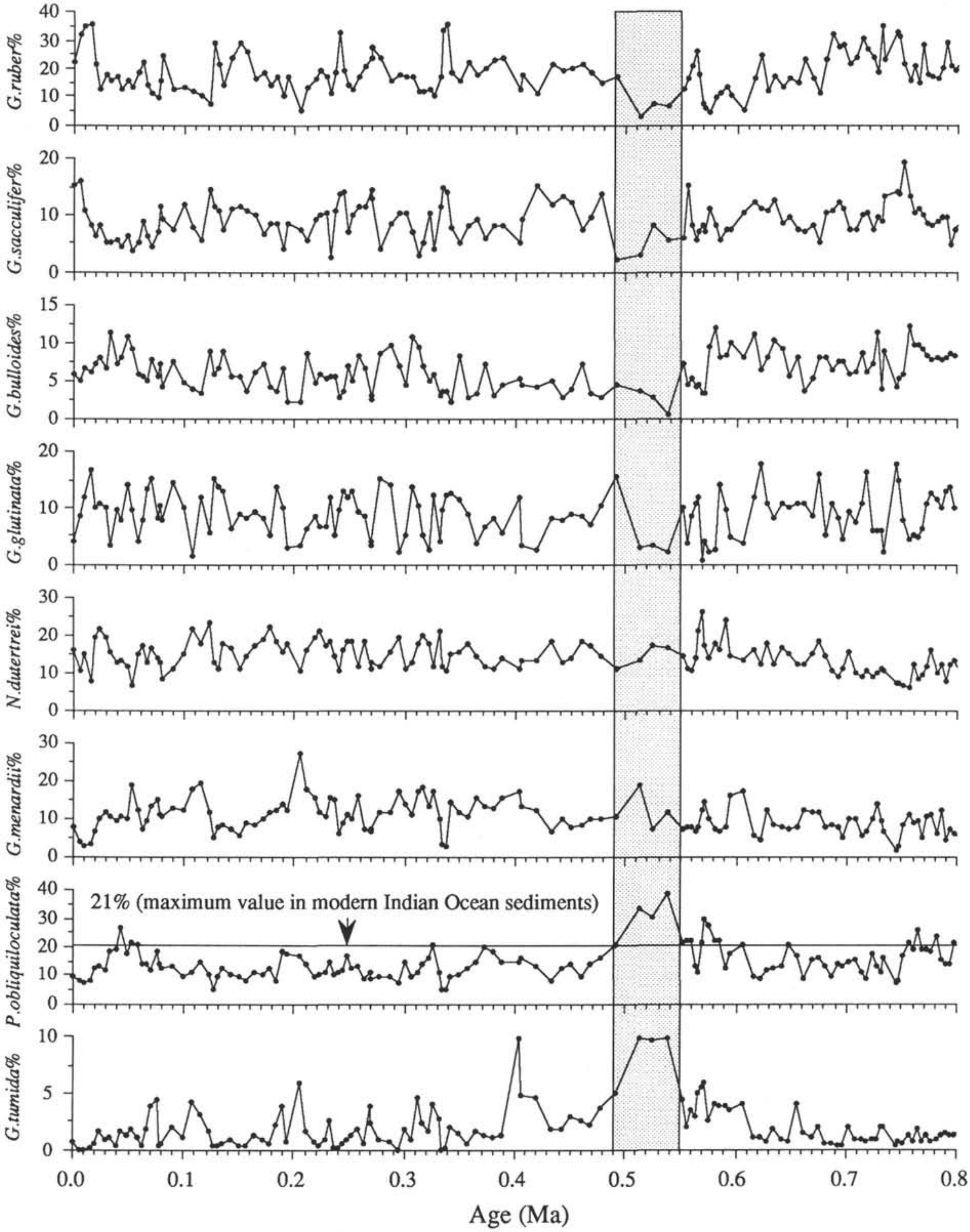

Figure 2. Percentage abundance of the eight major species of planktonic foraminifers plotted vs. age. The shaded region (490–550 ka) identifies a time of enhanced $CaCO_3$ dissolution characterized by low abundances of *G. ruber*, *G. sacculifer*, *G. bulloides*, *G. glutinata*, and high abundances of *G. menardii*, *P. obliquiloculata*, *G. tumida*. The maximum value (21%) of *P. obliquiloculata* observed in modern sediments from the Indian Ocean is marked by an arrow.

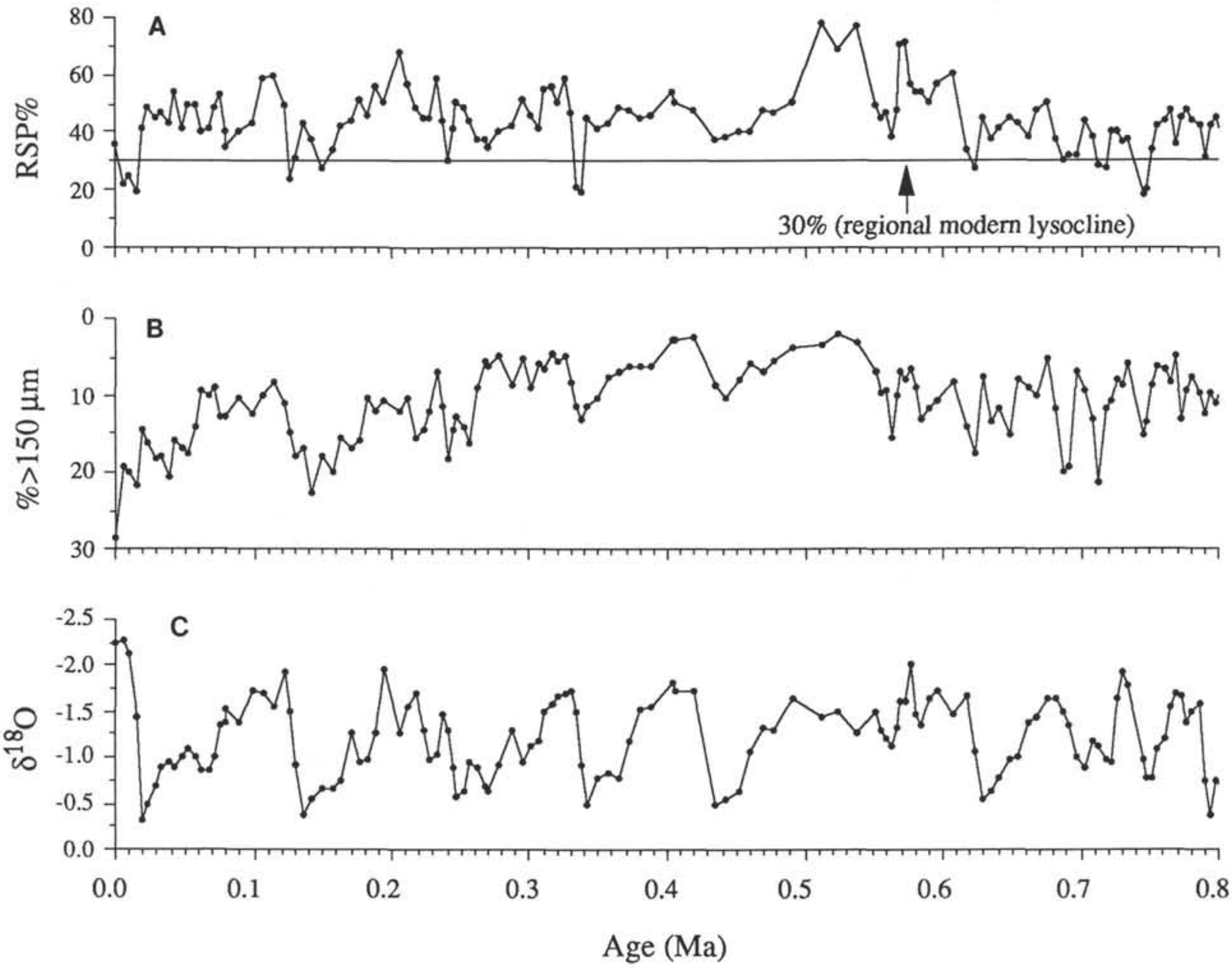

Figure 3. Percentage abundance of **A.** Resistant species ratio (RSP%). Arrow shows the modern foraminifer lysocline as defined by the 30% RSP level (see text for explanation). **B.** Coarse fraction (wt%>150 µm), and **C.** $\delta^{18}O$ (‰ to PDB of *G. sacculifer* from the 300–355 µm size range) from Site 758 plotted against age.

since species of similar susceptibility to dissolution show a common pattern. Between 490 and 550 ka, the relative percentages of susceptible species *G. ruber, G. sacculifer, G. bulloides,* and *G. glutinata* were significantly reduced while the abundances of the resistant species *P. obliquiloculata, G. menardii,* and *G. tumida* increased. This time interval is considered the mid-point of a long-term dissolution trend. The trend is also clearly observed in the RSP%, the coarse fraction record, and in the downcore abundance record of *G. tumida.* The dissolution trend is the "Brunhes Dissolution Cycle" first described in sedimentary records from the equatorial Pacific (Adelseck, 1977). This cycle has been observed in other Indian Ocean records in water depths ranging from 533 m (Cullen and Droxler, 1990; Droxler et al., 1990) to over 4000 m (Peterson and Prell, 1985b). The cause of the cycle is unknown but has been related to forces both internal (Pisias and Rea, 1988) and external (Jansen et al., 1986) to the climate system.

Ecological Factors Influencing Faunal Assemblages

The relative abundance of planktonic foraminifers distributed on the seafloor is determined not only by dissolution, but also by the ecology of the overlying surface waters. Numerous studies have documented the great utility of planktonic foraminifers in paleoecological reconstructions. In sediments which have not been significantly altered by $CaCO_3$ dissolution, variations in foraminifer faunal assemblages have been related to surface water conditions (Imbrie and Kipp, 1971; Cullen, 1984). The most important factors controlling foraminifer paleoecology include sea-surface temperature, salinity, and biological productivity.

As previously discussed, the SST in the Bay of Bengal is nearly constant on an annual basis. In addition, the SST during the last glacial maximum (LGM), ~18,000 years ago, was nearly the same as it is today. Reconstructions indicate a cooling of SST at the LGM of no more than 1°C in this area (CLIMAP, 1976; 1981; Prell et al., 1980; Cullen, 1981). The low seasonality in modern SST, and the stable response of SST to glacial-interglacial cycles suggests that SST was probably not a major influence on faunal variation at Site 758.

Past changes in the salinity gradient in the Bay of Bengal have been reconstructed along north-south transects based on planktonic foraminifer isotopes (Duplessy, 1982) and on faunal variations (Cullen, 1981). The faunal proxy of the salinity gradient was reconstructed along 90°E from 5°S to 20°N at three time intervals: the LGM; the middle of the transition (MT) from the LGM to the Holocene near 9 ka; and the Holocene (Cullen, 1981). During the LGM, the salinity gradient was weakened by an increase in salinity in the northern reaches of the Bay of Bengal. During the MT, the gradient was enhanced due to a freshening of

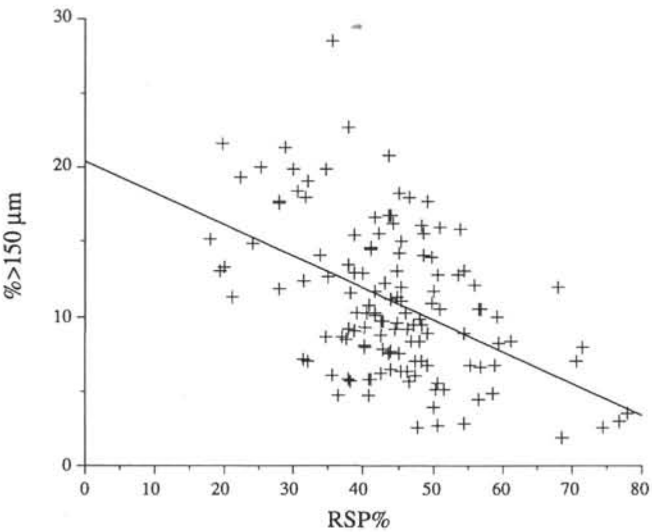

Figure 4. Scatter diagram of RSP% vs. coarse fraction. Enhanced dissolution is characterized by high RSP% values which are associated with low coarse fraction values.

waters in the north. In the Holocene, the salinity gradient was similar to that observed in the modern Bay of Bengal. The changes in the north were attributed to fluctuations in monsoonal precipitation and riverine input of fresh water (Cullen, 1981). The high salinity during the LGM was attributed to a reduction of monsoonal precipitation and riverine input. Likewise, the low salinity during the MT was attributed to an increase in precipitation and riverine input. Except for a brief period near the MT, the salinity in the southern Bay of Bengal (~5°N) has remained relatively stable at values between 33.5‰ and 34.0‰. Between the LGM and the MT, the salinity of the waters above Site 758 increased to about 34.5‰ (Figure 20 in Cullen, 1981). This somewhat higher salinity in the central Bay of Bengal was attributed to an increase in the eastward advection of high salinity water carried by the Southwest Monsoon Current, which in turn was related to a stronger summer monsoon (Cullen, 1981). The largest change in salinity occurred in the northern part of the Bay of Bengal. Salinity at Site 758 was probably not directly affected by riverine input as the site is located far from the coasts. Changes in intensity of the Southwest Monsoon Current, however, may have had an effect on the salinity of the waters above Site 758. The degree to which the salinity may have changed over Site 758 and the ecological response of the foraminifers are discussed below.

If biological productivity at Site 758 changed significantly over the past 800 k.y., it most likely changed in response to variations in the upwelling of nutrient-rich waters. Upwelling at Site 758 is presently minimal. The site is away from the upwelling regions associated with the equatorial divergence and with coastal upwelling zones in the Andaman Sea and off the coast of Sumatra. In Holocene and LGM sediments, variations in productivity related to upwelling intensity have been identified in the Andaman Sea and the northeastern Bay of Bengal (Fontugne and Duplessy, 1986). Greater organic carbon accumulation during the LGM was interpreted as indicating greater productivity and upwelling, which in turn was related to intensification of the Northeast monsoon. Only minor amounts of siliceous microfossils, which are considered an indication of upwelling and enhanced productivity, occur in the Quaternary sediments at Site 758 (Shipboard Scientific Party, 1989).

Ecological Change at Site 758

Having demonstrated that the late Quaternary faunal change at Site 758 is mainly controlled by the variation of $CaCO_3$ dissolution, a dissolution-buffered strategy has to be used to extract the ecological signal from the foraminifer abundance data. To minimize the effects of dissolution, which would increase the relative abundance of dissolution-resistant species at the expense of the susceptible species, we followed the method of Cullen (1981) and recalculated the percentage of three dissolution-resistant species *N. dutertrei, P. obliquiloculata,* and *G. menardii* (Fig. 6). This method allows us to examine ecological variations in abundance of *N. dutertrei, P. obliquiloculata,* and *G. menardii* on a dissolution-buffered basis because these three species have a similar resistance to dissolution.

In the recalculated abundances we observe large variations (10%–60%) in *N. dutertrei* which are superimposed on a long-term, but subtle increase of about 10% since at least 800 ka (Fig. 6A). The high amplitude fluctuations, which occurred on a time scale of 10–50 k.y., were most common between 0 and 600 ka. We attribute these patterns to ecological factors which may reflect environmental change in the surface waters above Site 758. Two ecological factors have been associated with the abundance of *N. dutertrei* in surface sediment samples. In the North Indian Ocean, high abundances of *N. dutertrei* appear closely linked to low sea-surface salinity (Cullen, 1981). Alternatively, high abundances of *N. dutertrei* in the eastern tropical Pacific (Berger, 1973) and in the Arabian Sea (Cullen, 1981) have been interpreted as indicating a shallow thermocline, a high nutrient level, and thus high productivity. To remove the dissolution imprint from the modern faunal abundance data (Prell, 1985) and to extract the ecologically controlled pattern of *N. dutertrei,* we recalculated the *N. dutertrei* percentage within three dissolution-resistant species *P. obliquiloculata, G. menardii,* and *N. dutertrei* (Fig. 7). This recalculation was identical to that performed on the downcore samples from Site 758. The core top values shown in Figure 7 are those in which the original sum of *P. obliquiloculata, G. menardii,* and *N. dutertrei* is greater than 30%. This level was chosen to avoid core tops with low abundances of these three species. Low abundances result in relative proportions which are not statistically significant.

High abundances of *N. dutertrei* in core tops are observed beneath waters with lowest salinities (<34‰) in the northern Bay of Bengal, in the Andaman Sea, and off Sumatra Coast. Lowest abundances of *N. dutertrei* were observed in the Arabian Sea where salinity exceeds 36‰. Based on this observation, a simple interpretation of the increase in the abundance of *N. dutertrei* with time is a long-term decrease in salinity at Site 758. Likewise, the large amplitude and high frequency fluctuations in the abundance of *N. dutertrei* may reflect relatively large and abrupt changes in salinity. Due to the great distance between Site 758 and the coast, it is unlikely that river run-off into the northern Bay of Bengal directly affected the salinity of the surface waters in the southern Bay of Bengal. A reduction in the salinity near Site 758 may have resulted from an increase in the advection of low salinity waters from the east through the Lombok Strait in response to a strengthening of the Southeast Asian Monsoon (Murray and Arief, 1988). Alternatively, there may have been a decrease in the advection of high salinity waters from the west by the Southwest Monsoon Current due to a weakening of the Southwest Monsoon. Finally, the salinity at Site 758 may have changed in response to regional fluctuations in the ratio of evaporation to precipitation.

We also observe a high concentration of *N. dutertrei* in core tops from regions where the thermocline shoals and upwelling of nutrient-rich water occurs. *N. dutertrei* is numerous in the central

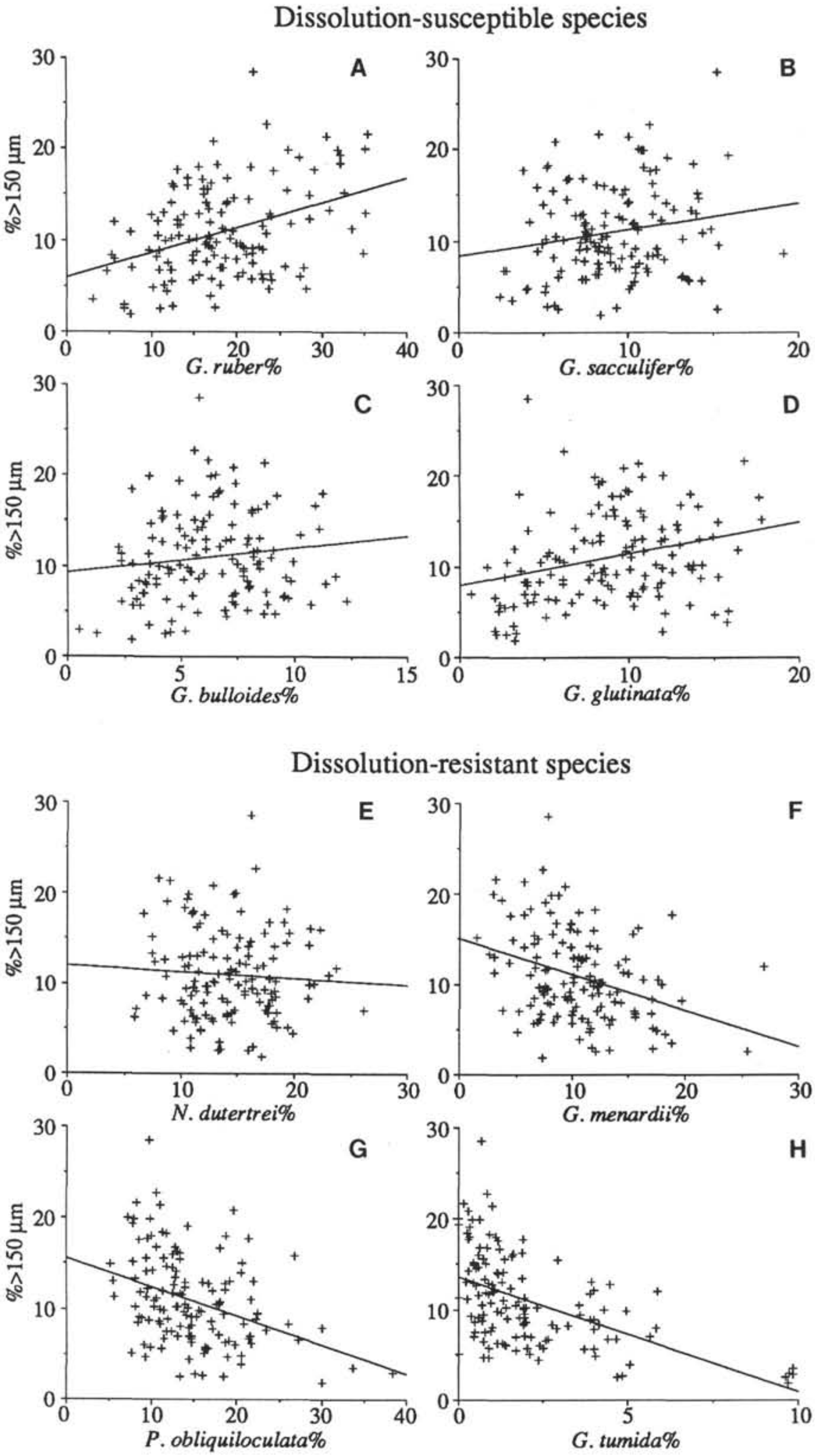

Figure 5. Scatter diagrams of coarse fraction vs. percentages of dissolution-susceptible species: **A.** *G. ruber*. **B.** *G. sacculifer*. **C.** *G. bulloides*. **D.** *G. glutinata*. Dissolution-resistant species: **E.** *N. dutertrei*. **F.** *G. menardii*. **G.** *P. obliquiloculata*. **H.** *G. tumida*. The lines are simple linear regressions. These plots show the relationships between foraminifer abundances and dissolution intensity. Strong dissolution is characterized by low coarse fraction and low percentages of dissolution-susceptible species (**A–D**). Enhanced preservation is characterized by high coarse fraction and low percentages of dissolution-resistant species (**E–H**).

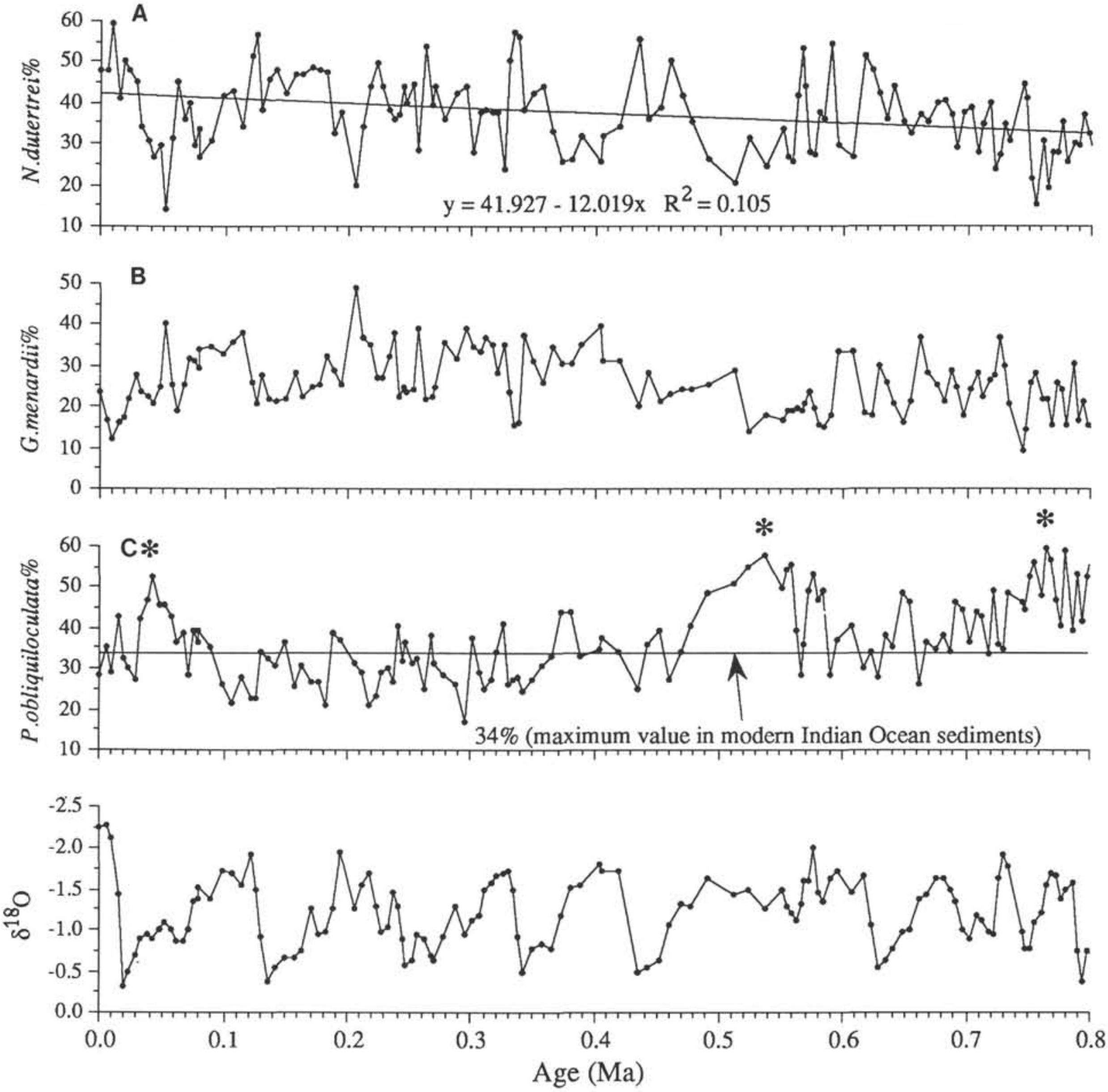

Figure 6. Recalculated percentage abundances of three dissolution-resistant species **A.** *N. dutertrei*. **B.** *G. menardii*. **C.** *P. obliquiloculata* plotted against age. The line in **A** is a simple linear regression which shows a 10% increase in *N. dutertrei* since 800 ka. For comparison to downcore values, the arrow in **C** shows the maximum surface sediment abundance (34%) of *P. obliquiloculata* from Prell (1985) in terms of recalculated percentage abundances (see text for discussion). Samples at 43 ka, 538 ka, and 765 ka contain anomalously high *P. obliquiloculata* abundances and are marked with a "*".

and south tropical Indian Ocean underneath the North and South Equatorial Current where there is a strong equatorial divergence (Fig. 7). High concentrations of *N. dutertrei* are also observed in the regions of coastal upwelling in the Andaman Sea and Sumatra Coast (Fig. 7). The intensity of this coastal upwelling may be controlled by the strength of the Northeast Monsoon (Fontugne and Duplessy 1986). Based on this observation, changes in the abundance of *N. dutertrei* over time at Site 758 could be explained by fluctuations in productivity. These changes may be linked to the intensity of the Northeast Monsoon or the strength of the equatorial divergence.

A second intriguing ecological pattern observed in the Site 758 record is the anomalously high abundances of *P. obliquiloculata*. Several downcore samples from Site 758 have abundances of *P. obliquiloculata* that are much greater than the abundances observed in all (290) core top samples from the Indian Ocean (Prell, 1985). The downcore samples have greater abundances when calculated either as a percentage of all 27 species (Fig. 2) or recalculated as a percentage of the three dissolution resistant species (*P. obliquiloculata, G. menardii,* and *N. dutertrei*) (Fig. 6C). This indicates that $CaCO_3$ preservation is not controlling the anomalously high abundances. For example, the highest abundance of *P. obliquiloculata* in core tops from the Indian Ocean occurs off the Sumatra Coast where values reach 21% (database from Prell, 1985) (Table 2). When recalculated as a percentage of only the dissolution resistant species, the *P. obliquiloculata* percentages in surface sediments are as high as 34%. In the record from Site 758, the percentage of *P. obliquiloculata* with respect to the entire fauna exceeds the surface sediment values during interglacial $\delta^{18}O$ stages 3, 13, 14, 15, and 21 (Fig. 2). Likewise,

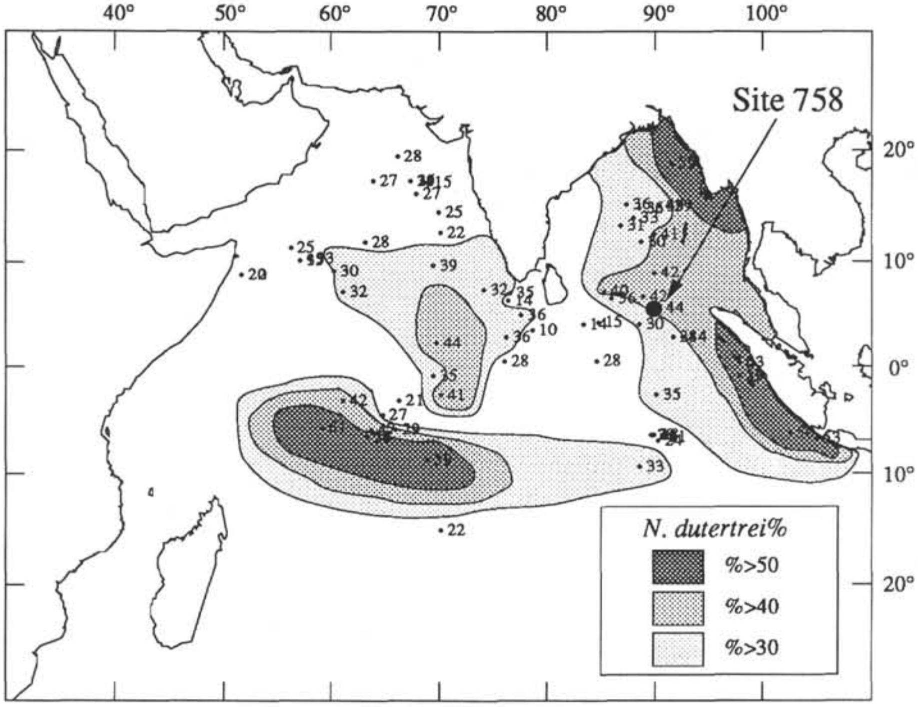

Figure 7. Spatial distribution of the recalculated abundance of *N. dutertrei* in core top samples from the north Indian Ocean (database from Prell, 1985). High abundances are distributed in the Andaman Sea, off the Sumatra Coast, and beneath strong equatorial current systems of the tropical Indian Ocean.

when examined on the dissolution-buffered basis, the recalculated percentage of *P. obliquiloculata* abundances in Site 758 often exceeds the recalculated core top value of 34% (Fig. 6C). High abundances of *P. obliquiloculata* in downcore samples at Site 758 are, however, similar to the high abundances observed in core tops from the western tropical Pacific (Cullen and Prell, 1984).

We compared the faunal compositions of the core tops from the tropical Indo-Pacific with three representative downcore samples from Site 758 which have anomalously high abundances of *P. obliquiloculata* (samples from $\delta^{18}O$ stage 3, 14, 21 that are marked with an "*" in Fig. 6C). First, we recalculate the core top database (Prell, 1985) in terms of the three dissolution-resistant (*P. obliquiloculata, G. menardii, and N. dutertrei*) species. Second, we calculated the dissimilarity coefficient (using a squared chord distance) between the core top samples and the three downcore samples. In Figure 8, we observe a low dissimilarity between the core top samples from the western tropical Pacific and the downcore samples from Site 758. We assume that similar faunas inhabit similar environments. Based on this assumption, the similarity of the core tops from the Pacific with the downcore samples suggests that surface water conditions in the modern western tropical Pacific were analogous to those in the northeastern Indian Ocean at certain times in the past. One possible explanation for the similar conditions during these times, is an increase in the advection of warm surface waters through the Indonesian Archipelago and into the northeastern Indian Ocean. This contention is supported by the observation of generally higher percentages of *P. obliquiloculata* during interglacials, when the throughflow between the tropical Indian and Pacific Oceans was probably greatest. During glacial times, low stands of the sea most likely restricted the exchange of water between these two regions. Alternatively, local oceanographic and climatic factors, such as the depth of the thermocline and the ratio of evaporation to precipitation, may have produced surface water conditions in the northeastern Indian Ocean that were similar to those presently found in the western tropical Pacific.

CONCLUSIONS

1. Over the past 800 k.y., variations in the relative abundance of planktonic foraminifers at Site 758 were predominantly controlled by fluctuations in $CaCO_3$ dissolution.

2. Dissolution varied at a cyclicity of ~100 k.y., in step with glacial/interglacial fluctuations. $CaCO_3$ preservation was generally good during glacial intervals and poor during interglacials. Greatest preservation occurred on climate transitions from glacials to interglacials.

3. The ~100 k.y. cycles are superimposed upon a long-term Brunhes Dissolution Cycle. The mid-point of this cycle, where dissolution was greatest, is centered between 400 and 550 ka and is bounded by strong preservation at 25 and 750 ka.

4. Variations in the dissolution-buffered abundance of *N. dutertrei* are attributed to ecological factors, most likely a decrease in sea-surface salinity or an increase in productivity.

5. The abundances of *P. obliquiloculata* in several downcore samples from Site 758 are greater than the abundances observed in core top samples from the Indian Ocean, but are similar to those found in core tops from the western tropical Pacific. This suggests that surface water conditions in the modern tropical Pacific were similar to conditions in the northeastern Indian Ocean at certain times in the past.

ACKNOWLEDGMENTS

The authors are grateful to A. Martin for assistance with planktonic foraminifer taxonomy and to W. Kang and T. Saha for help with sample preparation. We thank R. C. Thunell and T. Patterson for constructive reviews. Our work has greatly benefitted from discussions with J. L. Cullen, W. Howard, D. W. Murray, W. L. Prell, and Kuo-Yen Wei. This research was supported by

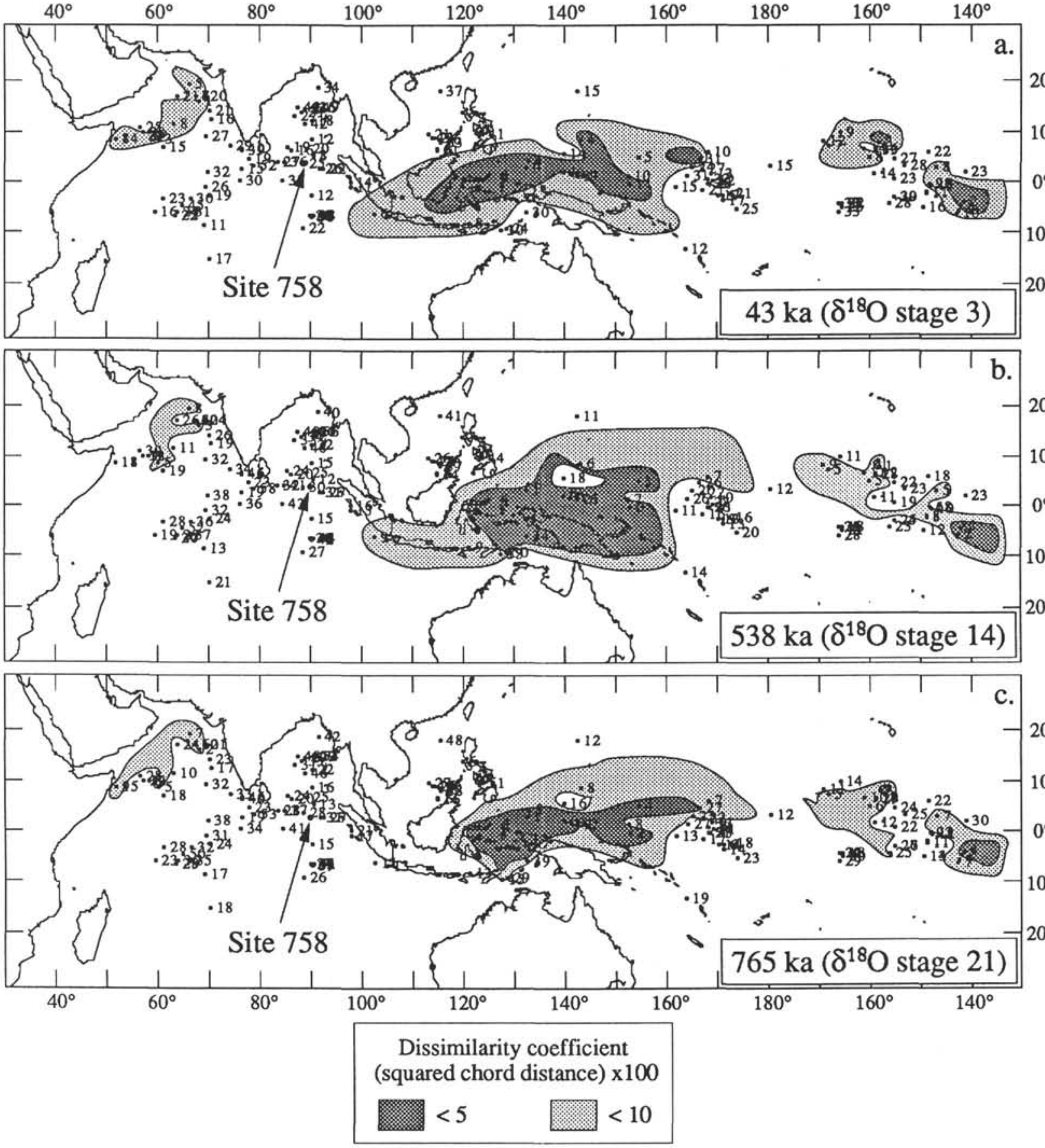

Figure 8. Spatial distribution of core top samples from the Indo-Pacific which contain foraminifer assemblages that are similar to the assemblages in three downcore samples (at ~43 ka, ~538 ka, and ~765 ka) from Site 758. The core top samples which are most similar to the three downcore samples are from the tropical western Pacific and are considered modern analogues of the downcore samples from Site 758. The modern analogues are indicated by the lowest dissimilarity coefficients and are mapped as the shaded regions.

grants from JOI/USSAC (TAMRF-20244) (J. W. Farrell and T. Janecek), NSF/OCE 8911874 (D. W. Murray and J. W. Farrell), and a Brown University Teaching Assistantship (1989–1990) awarded to Min-Te Chen.

REFERENCES

Adelseck, C. G., Jr., 1977. Recent and late Pleistocene sediments from the eastern equatorial Pacific Ocean: sedimentation and dissolution. [Ph.D. dissert.], Univ. of California, San Diego.

_______, 1978. Dissolution of deep sea carbonate: preliminary calibration of preservational and morphological aspects. *Deep-Sea Res.*, 24:1167–1185.

Bé, A.W.H., 1967. Foraminifera, families: *Globigerinidae* and *Globorotaliidae*, fiche No. 108. *In* Fraser, J. H. (Ed.), *Fiches d'Identification du Zooplancton.* Conseil Internat. l'Exploration Mer, Charlottenlund, Sheet 108.

Bé, A.W.H., and Hutson, W. H., 1977. Ecology of planktonic foraminifera and biogeographic patterns of life and fossil assemblages in the Indian Ocean. *Micropaleontology*, 27:369–414.

Bé, A.W.H., and Tolderlund, D. S., 1971. Distribution and ecology of living planktonic foraminifera in surface waters of the Atlantic and Indian Oceans. *In* Funnel, B. M., and Riedel, W. R. (Eds.), *The Micropaleontology of Oceans*, Cambridge (Cambridge Univ. Press), 105–149.

Berger, W. H., 1968. Planktonic foraminifera: selective solution and paleoclimatic interpretation. *Deep-Sea Res. Oceanogr. Abstr.*, 15: 31–43.

_______, 1970. Planktonic foraminifera: selective solution and the lysocline. *Mar. Geol.*, 8:111–138.

_______, 1973. Deep-sea carbonates: Pleistocene dissolution cycles. *J. Foraminiferal Res.*, 3:187–195.

_______, 1975. Deep-sea carbonates: dissolution profiles from foraminiferal preservation. *In* Sliter, W. V., Bé, A.W.H., and Berger, W. H. (Eds.), *Dissolution of Deep-Sea Carbonate*, Spec. Publ. Found. Foraminiferal Res., 13:82–86.

_______, 1979. Preservation of foraminifera. *In* Lipps, J. H. (Ed.), *Foraminifera Ecology and Paleoecology*. SEPM Short Course, 6:105–155.

Berger, W. H., Bonneau, M. -C., and Parker, F. L., 1982. Foraminifera on the deep-sea floor: lysocline and dissolution rate. *Oceanol. Acta*, 5:249–258.

CLIMAP project members, 1976. The surface of the ice-age Earth. *Science*, 191:1131–1137.

_______, 1981. Seasonal reconstructions of the Earth's surface at the last glacial maximum. *Geol. Soc. Am., Map and Chart Ser.*, MC36:1–18.

Colborn, J. G., 1975. The thermal structure of the Indian Ocean. *Internat. Indian Ocean Exped. Oceanogr. Monogr.*, 2:1–173.

Cullen, J. L., 1981. Microfossil evidence for changing salinity patterns in the Bay of Bengal over the last 20,000 years. *Palaeogeogr., Palaeoclimatol., Palaeoecol.*, 35:315–356.

_______, 1984. Climatic variation in the northern Indian Ocean: analysis of the distribution, ecology, and preservation of planktonic foraminifera in late Quaternary sediments. [Ph.D. dissert.], Brown Univ., Providence.

Cullen, J. L., and Droxler, A. W., 1990. Late Quaternary variations in planktonic foraminiferal faunas and pteropod preservation in the equatorial Indian Ocean: *In* Duncan, R. A., Backman, J., Peterson, L. C., et al., *Proc. ODP, Sci. Results*, 115: College Station, TX (Ocean Drilling Program), 579–588.

Cullen, J. L., and Prell, W. L., 1984. Planktonic foraminifera of the northern Indian Ocean: distribution and preservation in surface sediments. *Mar. Micropaleontol.*, 9:1–52.

Curray, J. R., and Moore, D. G., 1971. Growth of the Bengal deep-sea fan and denudation in the Himalayas. *Geol. Soc. Am. Bull.*, 82:563–572.

Droxler, A. W., Haddad, G. A., Mucciarone, D. A., and Cullen, J. L., 1990. Pliocene-Pleistocene aragonite cyclic variations in Holes 714A and 716B (The Maldives) compared with Hole 633A (the Bahamas): Records of climate-induced $CaCO_3$ preservation at intermediate-water depths. *In* Duncan, R. A., Backman, J., Peterson, L. C., et al., *Proc. ODP, Sci. Results*, 115: College Station, TX (Ocean Drilling Program), 539–577.

Duplessy, J.-C., 1982. Glacial to interglacial contrasts in the northern Indian Ocean. *Nature*, 295:494–498.

Fairbanks, R. G., Sverdlove, M., Free, R., Wiebe, P. H., and Bé, A.W.H., 1982. Vertical distribution and isotopic fractionation of living planktonic foraminifera from the Panama Basin. *Nature*, 298:841–844.

Fontugne, M. R., and Duplessy, J. -C., 1986. Variations of the monsoon regime during the upper Quaternary: evidence from carbon isotopic record of organic matter in North Indian Ocean sediment cores. *Palaeogeogr., Palaeoclimatol., Palaeoecol.*, 56:69–88.

Goldberg, E. D., and Griffin, J. J., 1970. The sediments of the northern Indian Ocean. *Deep-Sea Res. Oceanogr. Abstr.* 17:513–537.

Hutson, W. H., and Prell, W. L., 1980. A paleoecological transfer function, FI-2, for Indian Ocean planktonic foraminifera. *J. Paleontol.*, 54:381–399.

Imbrie, J., Hays, J. D., Martinson, D. G., McIntyre, A., Mix, A. C., Morley, J. J., Pisias, N. G., Prell, W. L., and Shackleton, N. J., 1984. The orbital theory of Pleistocene climate: support from a revised chronology of the marine $\delta^{18}O$ record. In Berger, A., Imbrie, J., Hays, H., Kukla, G., and Saltzman, B. (Eds.), *Milankovitch and Climate, Part I, Dordrecht (Reidel), 269–305.*

Imbrie, J. and Kipp, N. G., 1971. A new micropaleontological method for quantitative paleoclimatology: application to a late Pleistocene Caribbean core. *In* Turekian, K. K. (Ed.), *The Late Cenozoic Glacial Ages*, New Haven (Yale Univ. Press), 71–181.

Jansen, J.H.F., Kuijpers, A., Troelstra, S. R., 1986. A mid-Brunhes climatic event: long-term changes in global atmospheric and ocean circulation. *Science*, 232: 619–622.

Kipp, N. G., 1976. New transfer function for estimating past sea-surface conditions from sea-bed distribution of planktonic foraminiferal assemblages in the North Atlantic. *Mem. Geol. Soc. Am.*, 145:3–41.

Malmgren, B. A., 1983. Ranking of dissolution susceptibility of planktonic foraminifera at high latitudes of the south Atlantic Ocean. *Mar. Micropaleontol.*, 8:183–191.

Murray, S. P., and Arief, D., 1988. Throughflow into the Indian Ocean through the Lombok Strait, January 1985–January 1986. *Nature*, 333:444–447.

Parker, F. L., 1962. Planktonic foraminiferal species in Pacific sediments. *Micropaleontology*, 8:219–254.

Parker, F. L., and Berger, W. H., 1971. Faunal and solution patterns of planktonic foraminifera in surface sediments of the South Pacific. *Deep-Sea Res. Oceanogr. Abstr.*, 18:73–107.

Peterson, L. C., and Prell, W. L., 1985a. Carbonate dissolution in recent sediments of the eastern equatorial Indian Ocean: preservation patterns and carbonate loss above the lysocline. *Mar. Geol.*, 64:259–290.

_______, 1985b. Carbonate preservation and rates of climatic change: an 800 kyr record from the Indian Ocean. *In* Sundquist E. T., and Broecker, W. S. (Eds.), *The Carbon Cycle and Atmospheric CO_2: Natural Variations Archean to Present*, Washington (Am. Geophys. Union), 32:251–270.

Pisias, N. G., and Rea, D. K., 1988. Late Pleistocene paleoclimatology of the central equatorial Pacific: sea-surface response to the southeast tradewinds. *Paleoceanography*, 3:21–37.

Prell, W. L., 1984. Variation of monsoon upwelling: a response to changing solar radiation. *In* Hansen J. E., and Takahashi, T. (Eds.), *Climate Process and Climate Sensitivity*, Am. Geophys. Union, Maurice Ewing Ser., 29:48–57.

_______, 1985. The stability of low-latitude sea-surface temperature: an evaluation of the CLIMAP reconstruction with emphasis on the positive SST anomalies. *Dept. Energy Tech. Rept., TR-025.*

Prell, W. L. and Curry, W. B., 1981. Faunal and isotopic indices of monsoonal upwelling: western Arabian Sea. *Oceanol. Acta*, 4:91–98.

Prell, W. L., Hutson, W. H., Williams, D. F., Bé, A.W.H., Geitzenauer, R., and Molfino, B., 1980. Surface circulation of the Indian Ocean during the last glacial maximum, approximately 18,000 yr B.P., *Quat. Res.*, 14:309–336.

Prell, W. L., Imbrie, J., Martinson, D. G., Morley, J. J., Pisias, N. G., Shackleton, N. J., and Streeter, H. F., 1986. Graphic correlation of oxygen isotope stratigraphy: application to the late Quaternary. *Paleoceanography*, 1:137–162.

Prell, W. L., Marvil, R. E., and Luther, M. E., 1990. Variability in upwelling fields in the northwestern Indian Ocean 2. data-model comparison at 9000 years B.P. *Paleoceanography*, 5:447–457.

Ravelo, A. C., Fairbanks, R. G., and Philander, G., 1990. Reconstructing tropical Atlantic hydrography using planktonic foraminifera and an ocean model. *Paleoceanography*, 5:409–431.

Rodolfo, K. S., 1967. Sediments of the Andaman Sea, northeastern Indian Ocean. *Mar. Geol.*, 7:371–402.

Shackleton, N. J., and Opdyke, N. D., 1973. Oxygen isotope and paleomagnetic stratigraphy of equatorial Pacific core V28-238: oxygen isotope temperature and ice volumes on a 105 and 106 year scale. *Quat. Res.*, 3:39–55.

_______, 1976. Oxygen isotope and paleomagnetic stratigraphy of core V28-239, late Pliocene to latest Pleistocene. *In* Cline, R. M., and Hays, J. D. (Eds.), *Investigations of Late Quaternary Paleoceanography and Paleoclimatology*, Mem. Geol. Soc. Am., 145:449–464.

Shipboard Scientific Party, 1989. Site 758. *In* Peirce, J., Weissel, J., et al., *Proc. ODP, Init. Repts.* 121: College Station, TX (Ocean Drilling Program), 359–453.

Thompson, P. R., Bé, A.W.H., Duplessy, J. C., and Shackleton, N. J., 1979. Disappearance of pink-pigmented *Globigerinoides ruber* at 120,000 yr B.P. in the Indian and Pacific Oceans. *Nature*, 280:554–558.

Thunell, R. C., and Honjo, S., 1981a. Planktonic foraminiferal flux to the deep ocean: sediment trap results from the tropical Atlantic and the central Pacific. *Mar. Geol.*, 40:237–253.

_______, 1981b. Calcite dissolution and the modification of planktonic foraminiferal assemblages. *Mar. Micropaleontol.*, 6:169–182.

Thunell, R. C., and Reynolds, L. A., 1984. Sedimentation of planktonic foraminifera: seasonal changes in species flux in the Panama Basin. *Micropaleontology*, 30:243–262.

Wyrtki, K., 1973. Physical oceanography of the Indian Ocean. *In* Zeitzschel, B., and Gerlach, S. A. (Eds.), *The Biology of the Indian Ocean*, Vol 3: New York (Springer-Verlag), 18–36.

_______, 1988. Oceanography Atlas of the International Indian Ocean Expedition, New Delhi (Amerind).

Ms 121B-174
Date of initial receipt: 17 April 1990
Date of acceptance: 25 November 1990